CHALMERS
UNIVERSITY OF TECHNOLOGY

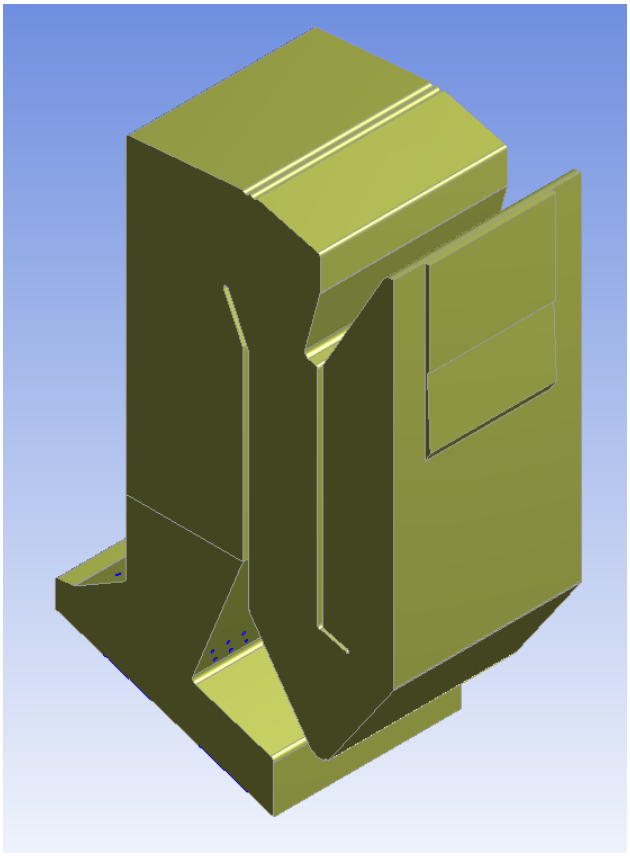

Sulfating of Alkali Chlorides in Waste-to-Energy

Master's thesis within the Innovative and Sustainable Chemical Engineering Programme

Oskar Sundborg
Albin Tärnåsen

Department of Space, Earth and Environment
CHALMERS UNIVERSITY OF TECHNOLOGY
Gothenburg, Sweden 2018

Master's thesis 2018:SEEX30

Sulfating of Alkali Chlorides in Waste-to-Energy

Oskar Sundborg
Albin Tärnåsen

CHALMERS
UNIVERSITY OF TECHNOLOGY

Department of Space, Earth and Environment
Division of Energy Technology
Chalmers University of Technology
Gothenburg, Sweden 2018

Sulfating of Alkali Chlorides in Waste-to-Energy
Oskar Sundborg
Albin Tärnåsen

Supervisors: Sven Andersson, Babcock & Wilcox Völund AB & Thomas Allgurén, Department of Space, Earth and Environment
Examiner: Klas Andersson, Department of Space, Earth and Environment

Master's Thesis 2018:SEEX30
Department of Space, Earth and Environment
Division of Energy Technology
Chalmers University of Technology
SE-412 96 Gothenburg
Telephone +46 31 772 1000

Cover: Geometry of the Renova boiler constructed in Fluent.

Typeset in LaTeX
Printed by Chalmers Reproservice
Gothenburg, Sweden 2018

Sulfating of Alkali Chlorides in Waste-to-Energy
Oskar Sundborg & Albin Tärnåsen
Department of Space, Earth and Environment
Chalmers University of Technology

Abstract

This thesis work involved the sulfation of alkali chlorides in Waste-to-Energy boilers. Sulfation, and thus removal, of these alkali chlorides is important since it can reduce high temperature corrosion and dioxin formation in the boiler. The objective was to investigate the impact that different properties such as temperature and composition have on the degree of sulfation, i.e. the fraction of alkali chlorides that have been sulfated. Two softwares were mainly used in this thesis work, namely Fluent and CHEMKIN. Fluent was used for a CFD-analysis to estimate the cooling rate and residence time of the flue gas in one of the investigated boilers and CHEMKIN was then used to simulate the course of sulfation in 1D. The results from the CFD-analysis proved to be insufficient due to the simplifications made. However, with the addition of a fictional flame the cooling rate could be estimated. The cooling rate could then be compared with a more realistic cooling rate and could thus be validated as a realistic representative. The residence time from the CFD-analysis was deemed to be realistic without any further actions. With the information gathered from the CFD-analysis, the kinetic simulations could be commenced in CHEMKIN. The results from these simulations show that it is possible to predict the degree of sulfation fairly well in both investigated boilers individually by adjusting parameters e.g. for mixing and carbon monoxide combustion. In other words, a general model that can predict the degree of sulfation for all boilers was not achieved but rather a framework that requires individually adjusted parameters for each investigated boiler. The model did however generally follow the same trends as the reference data which suggests that the kinetics are valid. With the aid of the model it was found that the presence of sulfur, radicals and slower cooling rates was favourable for the sulfation while chlorine and calcium suppresses it. Some phenomena could not be accounted for completely due to limitations of the model, such as mixing and variations over time. Additionally, the behavior of the gaseous sulfur is disputable. Some believe that sulfur dioxide is the most important sulfur specie in the sulfation process whilst others believe it to be sulfur trioxide. This makes the injection of sulfur problematic to implement into the model.

Keywords: sulfation, alkali, chlorine, sulfur, sulfuric acid, waste-to-energy, waste, incineration, boiler, CFD, CHEMKIN.

Contents

List of Figures

List of Tables

1
Introduction

Flue gases from waste incineration contain corrosive salts such as alkali, i.e. mainly sodium- and potassium, chlorides. Due to the presence of these salts; the temperature must be limited in the superheaters of the Waste-to-Energy boilers to avoid excessively high corrosion rates. It is possible to reduce the amount of these corrosive salts by making them react with SO_2 to form less harmful compounds in the form of alkali sulfates [3]. This can be done either by introducing external sulfur or by recirculating the inherent sulfur in the fuel where the latter is called sulfur recirculation which was invented at Karlsruhe Insitute of Technology (KIT). It is currently marketed and sold by Babcock & Wilcox (B&W) Völund A/S which has a worldwide exclusive license. There are many kinetic studies that have contributed to the understanding of the kinetics relevant for sulfur recirculation. In this work, the mechanism by Hindiyarti et al. [2] will be used as a basis.

1.1 Background

Sulfur is commonly found in household waste and when the waste is burned, sulfur dioxide is formed. The sulfur dioxide can be converted into sulfuric acid and separated from the other gas components in the later stages of the flue gas treatment by addition of hydrogen peroxide in a wet scrubber. It can then be recirculated into the combustion chamber and there utilize the high temperature to react with the alkali chlorides. The formed alkali sulfates condense and form particles before reaching the superheaters while the alkali chlorides may condense on the superheater tubes. Not only are alkali sulfates less sticky, they are also less corrosive than the alkali chlorides. This may be utilized to obtain a higher work output in the steam turbine due to the potential increase in steam temperature since higher temperatures are allowed at the surface of the superheater tubes. Another advantageous option is to keep the low temperature and thus obtain a longer lifetime of the superheater tubes [4]. B&W Völund A/S are interested in utilizing sulfur recirculation since it can potentially improve their boilers. For this reason, there is a need for a model that can predict the reduction of alkali chlorides in their boilers.

1.2 Objective

The aim of this thesis work is to find the variables that affect the reduction of alkali chlorides by high temperature reactions with sulfur in Waste-to-Energy boilers. Two boilers will be investigated in the work; one at Renova in Gothenburg, Sweden and

one at Måbjerg Energy Center (MEC) in Holstebro, Denmark. A few examples of variables that will be tested are cooling rate, flame temperature and amount of hydrochloric acid in the flue gas. It will then be investigated how well the degree of sulfation can be predicted with 1-D simulations in CHEMKIN which is a one dimensional simulation software for chemical reactions. Additionally, an interim objective is to create a CFD-model of the boiler at Renova to investigate the cooling rate and residence time of the flue gas. This information is used as input to the succeeding 1D modelling in CHEMKIN.

1.3 Sources of data

Two main sources of data were used in this thesis work. Firstly; a sulfation study that was conducted by Andersson et al. [3] provided fly ash compositions and process variables during the time periods of different injections of sulfuric acid in the Renova boiler. This data consisted of nine cases; three without injection (Case 1-3), three with intermediate injection (Case 4-6) and three with full injection (Case 7-9). Similar experiments have been conducted for the MEC boiler which is roughly half the size of the boiler at Renova and utilizes sulfur recirculation since 2016. The exceptions are that there were six cases instead of nine; three without injection (Case 1-3) and three with injection (Case 4-6). Also, there were no process variables and amount of injection available which made it necessary to make additional assumptions for the MEC boiler. Secondly, a visit to Renova was made in order to gather the data necessary to set up a CFD-model. This data included both geometrical and year-averaged process data, such as flow rates, stack compositions and temperatures. The boiler at MEC has already been simulated in CFD by B&W Völund A/S and the results from this study was available through a confidential technical report.

2
Theory

In this chapter the theory of the sulfation process will be presented along with a description of the relevant kinetics.

2.1 Sulfation of alkali chlorides

Sulfation is the process in which a salt is converted to a sulfated salt, i.e. the anion in the substance becomes a sulfate ion. The involved mechanics will differ depending on the salt which is sulfated. In this thesis work however, the focus will be on the sulfation of alkali chlorides and particularly on the sulfation of potassium. Many studies have been made to investigate the sulfation of potassium, since it is of great importance when it comes to high temperature corrosion (HTC) of boilers. The particular interest in potassium comes from its dominant role for the HTC in many fuels, compared to other HTC-inducing substances such as sodium which usually have a lower concentration than potassium. This is the case for many bio-based fuels such as wood and straw [2][5]. Municipal waste on the other hand generally contains more sodium and calcium than potassium [6]. This is one of the greatest challenges with this thesis work since the kinetics of the sulfation of sodium and calcium are not so well documented. It has however, been proposed that sodium follows a similar reaction mechanism to that of potassium [2]. Due to this, the sulfation of the sodium will be represented by the kinetics of potassium and all references to potassium in this work hereinafter include sodium as well.

Very little seems to be known about the impact that calcium has on the sulfation of potassium and sodium. There are however some information one can use to get indications of how calcium behaves through the course of the sulfation process. It is for example fairly certain that no calcium chloride will be present during the sulfation process since calcium chloride is very keen to oxidize at the high temperatures present in the boiler (>800K) [7]. The same applies for calcium carbonate [8]. For this reason, it is probable that most calcium will be released from the fuel in the form of either calcium oxide or calcium sulfate. The conversion of calcium sulfate from calcium oxide is found by Seehra and Gopalakrishnan [8] to be occurring through particle diffusion at rates that are negligible for the circumstances within this work. Due to the lack of knowledge, the calcium salts are treated as inert in the simulations and their kinetics are therefore not implemented into CHEMKIN. The calcium salts are however assumed to affect the inlet conditions since they contain oxygen and/or sulfur and thus reduce those elements from the flue gas.

2.2 Degree of sulfation

The degree of sulfation (D.o.S.) can be defined as the conversion of potassium- and sodium chloride to potassium- and sodium sulfate. The definition is shown in equation 2.1 below. The reason why calcium is not included in this definition is because calcium chloride is of less importance when it comes to preventing HTC since it is, as stated before, probably not present at the high temperatures of the boiler.

$$\text{D.o.S.} = \frac{2 * (x_{\text{K}_2\text{SO}_4,\text{fly ash}} + x_{\text{Na}_2\text{SO}_4\text{fly ash}})}{x_{\text{K,fly ash}} + x_{\text{Na,fly ash}}} \tag{2.1}$$

Where x denotes the mole fraction. The total amount of potassium and sodium in the fly ash can be seen in the denominator, this is the same as the initial amount of potassium and sodium chlorides since it is assumed that all potassium and sodium leaves the fuel as chlorides. The reason for the multiplication of two in the numerator is that there are two potassium and sodium atoms in each potassium and sodium sulfate.

A widely used measure for the degree of sulfation in Waste-to-Energy contexts is the chlorine to sulfur ratio. The advantage of the chlorine to sulfur ratio is that it can be measured in the fly ash and that it is relatable to the degree of sulfation. The more chlorine compared to sulfur that exists in the fly ash; the less sulfation has occurred. This is due to the fact that all alkali, except for the alkali that goes to the bottom ash, will end up in the fly ash while the sulfur and chlorine can either end up in the fly ash (bonded to metals) or in the flue gas as sulfur oxides and hydrochloric acid. The amount of chlorine and sulfur in the fly ash is therefore a good indication of how much alkali chlorides that have been sulfated.

2.3 Kinetics

Kinetic mechanisms for the gas phase reactions involved in the sulfation of potassium chloride have been proposed by Hindiyarti et al. [2]. This work will be used as the basis for this work. The suggested reaction pathway can be seen in Figure 2.1 below. The kinetics are implemented into CHEMKIN in the form of Arrhenius constants and activation energies. Additionally thermodynamic data is implemented to account for the equilibria of the reactions. There have been propositions both that the sulfation process occurs through surface reactions in a heterogeneous pathway [9] and that the sulfation reactions occurs much faster in the gaseous phase with a homogeneous pathway [2][10]. Only the kinetics for the homogeneous gas phase reactions will be simulated in this work since this is generally the supported theory in the more recent studies [2][10][1].

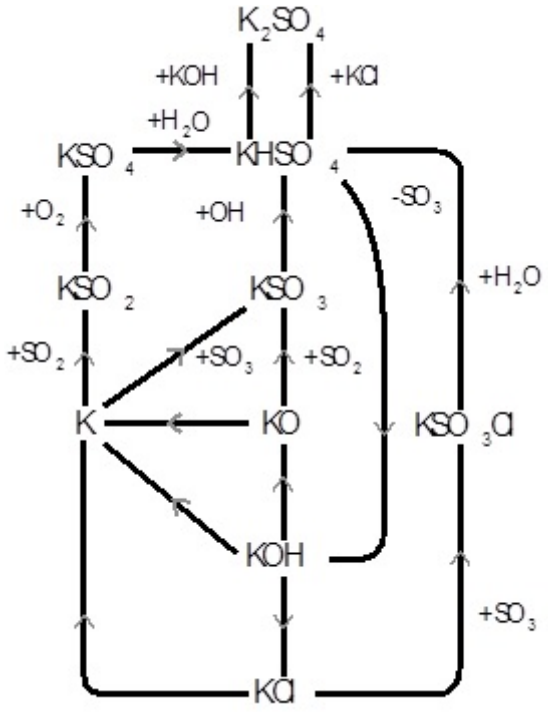

Figure 2.1: Reaction pathway used in this work. Figure made by Allgurén [1] using kinetic mechanisms by Hindiyarti et al. [2].

3

Method

In this chapter, the methods which were used to obtain the results are presented and discussed. The general approach can be seen in Figure 3.1 below and was as follows. Data was gathered from Renova and refined in order to start creating the CFD-model. When the CFD-model had been completed information about residence times and temperature profiles could be obtained. This information could then be analyzed and processed in MATLAB so that it could be utilized in CHEMKIN. The results from the CHEMKIN simulations was then compared with experimental data and the correlation between them was investigated. For the MEC b oiler a CFD-model was available and the data could be processed in MATLAB directly. Similarly to Renova, MEC had raw process data that required refinement before the CHEMKIN simulations could be done. For in-depth details regarding this chapter, refer to the appendix.

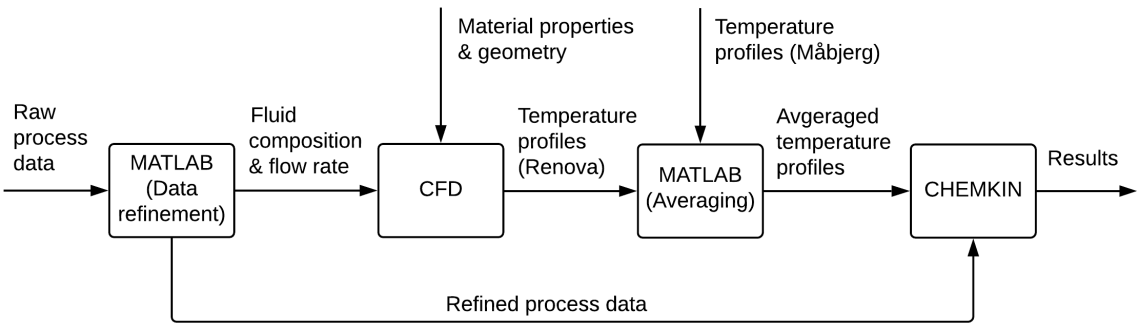

Figure 3.1: Simplified flow chart of the methodology.

3.1 Refining process data from Renova

In order to conduct a CFD analysis to obtain a preliminary temperature profile and residence time distribution in the boiler, sufficient data for the flows was needed. These data were gathered from the collection of historically monitored data for the Renova boiler. A flowchart of this boiler and its flue gas aftertreatment system is shown in Figure 3.2 below.

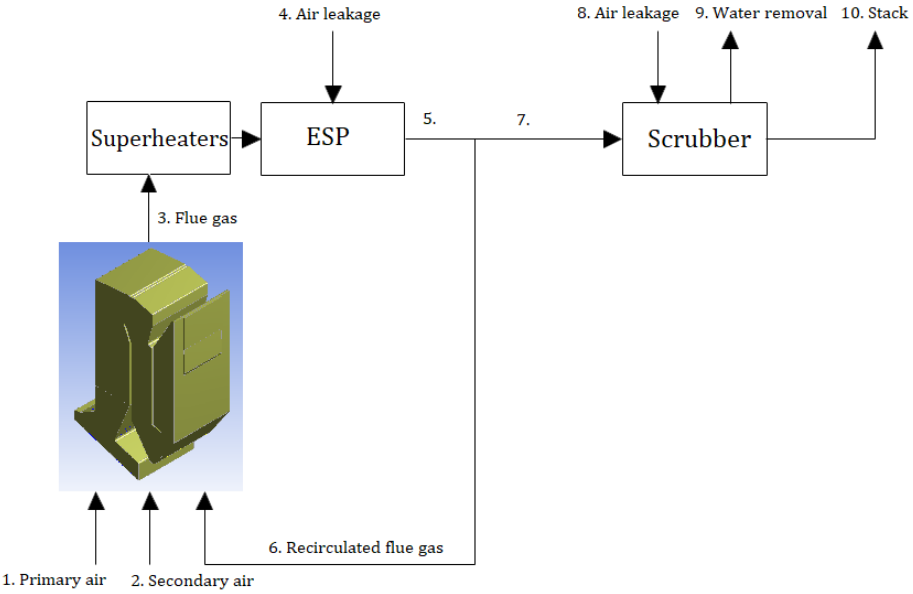

Figure 3.2: Overview of the Renova boiler and the flue gas aftertreatment system. Only the units and streams that affect the flue gas properties are included.

The collected process data consisted of flow rates and compositions of various flows, which can be found in Table A.1. The unknown flow rates and compositions were then calculated with balances and iterations. Because the system is over-specified with one value, something had to be neglected. The nitrogen concentration in the outlet can be calculated by substituting all known mole fractions from one but this was chosen to be neglected because it can instead serve as a validation when the nitrogen concentration is calculated elsewhere. To make sure that the measurements are reliable, two additional validations were made. Firstly; the highest temperature at which the flue gas should reach in order to release the correct amount of heat was calculated to about 1500 K, see Appendix B.1.3 for the calculation. However, this is the peak temperature of the flue gas assuming no heat would be produced in the flame. It should therefore be lower in the simulations which is implemented and accounted for in Section 3.3. This agrees well with the temperature profiles provided from CFD-simulations of the boiler at MEC and the profiles are shown in Figure 3.5. Secondly; assuming a total waste flow of 22 tonnes per hour, the moisture content in the solid waste was calculated to 48.72 wt%, see Appendix B.1.4 for the calculation. This is a realistic scenario since a study of waste that have been stored on a landfill shows a moisture content that ranges between 34 and 48 wt% [11].

The assumptions for the balance equations were as follows. All molecules entering the gas from the combustion comes from reactions with hydrocarbons and moisture. The remaining reactions are assumed to produce ash and particles that do not take up any volume in the gas. The gas is assumed to contain only nitrogen, oxygen, water vapour and carbon dioxide since the other species have much lower concentrations. Additionally, it is assumed that water is condensed out of the system in the scrubber and that air leaks into the system in the electrostatic precipitator filter (ESP) and in the scrubber which can be seen in the flowchart in Figure 3.2. The

ESP removes the fly ash which contains the remaining alkali and calcium after the bottom ash.

3.2 CFD-analysis

A CFD-analysis was conducted in ANSYS Fluent in order to find out if realistic temperature curves and residence times can be simulated for the Renova boiler. The boiler in MEC has already been investigated with CFD and this analysis will serve as a tool for comparison. Due to time limitations, it was decided that the CFD-model should be kept as simple as possible. For this reason, no combustion was simulated which resulted in somewhat unrealistic temperature profiles at the inlet of the boiler. The remainder of this section will briefly go through the important assumptions in the CFD-simulation and what came out of it. A more thorough description of the CFD-analysis can be found in Appendix C.

The boiler was drawn according to schematics obtained from Renova along with information retrieved at an early visit to the plant. The secondary- and recirculated air is injected with 48 different side inlets with varying position and flow angle. They can be seen in Figure 3.3b below. The primary air is injected from the bottom of the boiler. After the geometry was complete, it was meshed with approximately 1.6 million tetrahedral cells, accounting for y^+ adaption as well as gradient adaptions based on velocity and temperature.

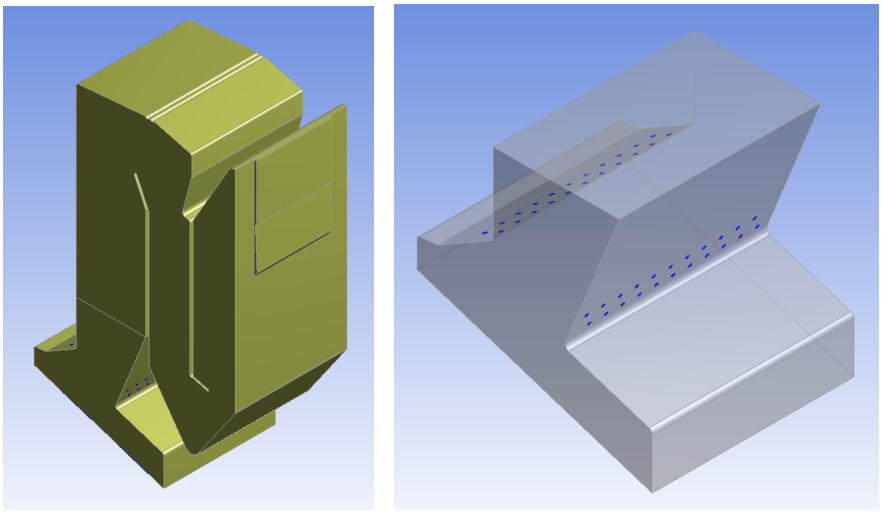

(a) The whole boiler. **(b)** The inlets of the boiler.

Figure 3.3: 3D Geometry of the boiler which was used in the CFD-model.

All inlets were set to the same temperature, 1484 K, thus fulfilling the energy balance, see Appendix B.1.3 for the equations used in the energy balance. This was done so that the high temperature is sustained longer in the zone where the combustion takes place. When adding the heat of reaction to the primary inlet temperature

only, the temperature decreased unrealistically abrupt but the velocity fields looked realistic. Figure 3.4a below shows the chosen solution with the heat of reaction distributed evenly among all inlets and Figure 3.4b shows the pathlines of the velocity magnitude in the boiler.

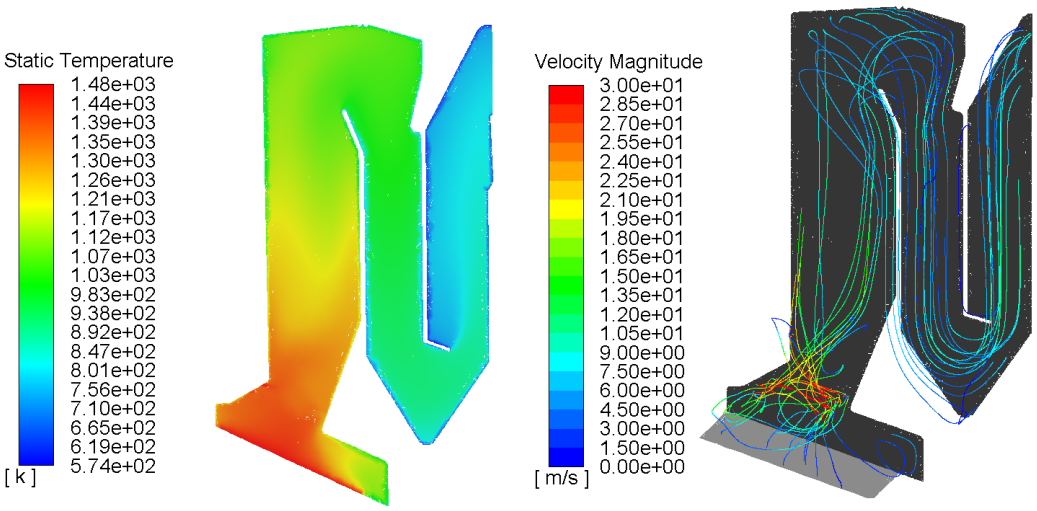

(a) Temperature in the Renova boiler. **(b)** Pathlines with the velocity magnitude for the Renova boiler.

Figure 3.4: Temperature and velocity magnitude of the flue gas according to the CFD-model.

The flows were set according to the calculated mass flows in Table A.1 in Appendix A, see Appendix B.1.2 for the equations used in the mass balances. The outer walls were set to a constant temperature according to the saturated water temperature at 50 bar. The walls were assumed to consist of a 5 mm thick steel layer as well as a deposit layer with a thickness that was varied until the desired outlet temperature of the boiler was reached. The walls of the first part of the boiler seen in Figure 3.3b had an additional 5 cm thick brick wall covering the steel to shield it from the intense heat and corrosion.

The fluid within the system was defined as air with some property changes to better fit the properties of the flue gas. The chosen turbulence model was the Realizable k-ε model and the radiation model was a discrete ordinates model with increased resolution. The emissivity of all surfaces were found and set [12][13] but the inlets were assumed to have no emissivity. The emissivity of the flue gas was estimated using a combination of the WSGG-model proposed by Johansson et al. [14] and a soot radiation model proposed by Gharehkhani et al. [15].

3.3 Refining temperature profiles

When investigating the temperature profiles from the CFD-simulations as described in Appendix D, it was soon discovered that the profiles have a very steep slope in

the beginning since no combustion is simulated, see Figure 3.5a below. The profiles produced for the boiler at MEC, which does simulate the combustion, has a very different appearance, as can be seen in Figure 3.5b below. When comparing the impact from each of these curves in CHEMKIN simulations it was discovered that the curve that does not include a flame cannot be used to predict a reasonable outcome. This is especially due to the fact that the injection point for sulfur dioxide will have a very different temperature which severely impacts the importance of the injection for the rate of sulfation. This can be seen by comparing the temperatures after 2.55 s in Figure 3.5 where the gas flow in the Renova boiler has a temperature of approximately 1160 K and the Måbjerg boiler approximately 1360 K. Such a great difference in temperature affects the rate of sulfation considerably.

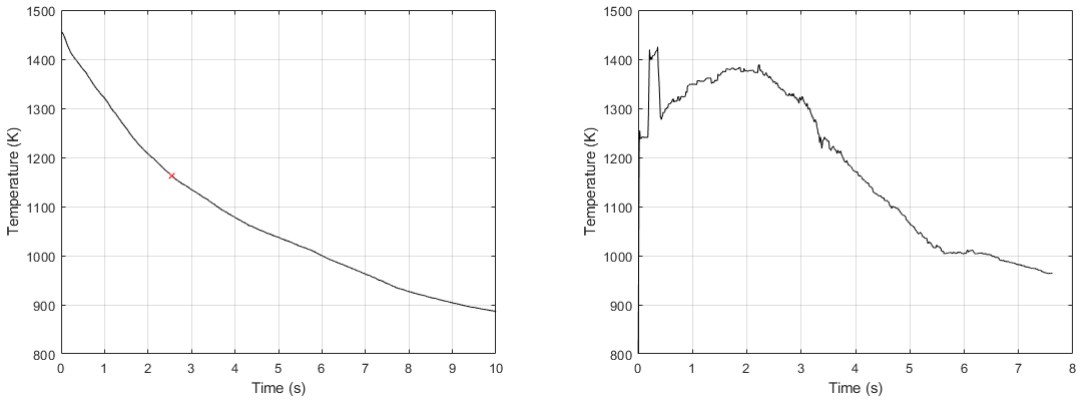

(a) Preliminary curve for the Renova boiler. The injection point at 2.55 seconds is shown with a red cross.

(b) Preliminary curve for the MEC boiler. The injection occurs at the inlet.

Figure 3.5: Temperature curve for the investigated boilers.

The temperature curves from the CFD-analysis were used to produce a representation of the heat transfer, i.e. radiation and convection. The temperature curve provided in Figure 3.5a could be fitted to an exponential decay equation. This regression model turned out to fit the temperature curve well if the decaying parameter is equal to the difference between the flue gas temperature and the wall temperature. The most accurate fit was found when the wall temperature was set to 230 K above the temperature of the boiling water, which results in a wall temperature (T_W) of 766.9 K, a value which agrees well with the average wall temperature in the CFD-model. The resulting model correspond to an inlet temperature of 1419 K (compared to 1455 K in Figure 3.5a) along with an exponential factor of -0.1778. The equation along with its parameters can be seen in Equation 3.1 below.

$$T(t) - T_W = (1419 - T_W) * e^{-0.1778t} \tag{3.1}$$

The result of the fit can be seen in Figure 3.6.

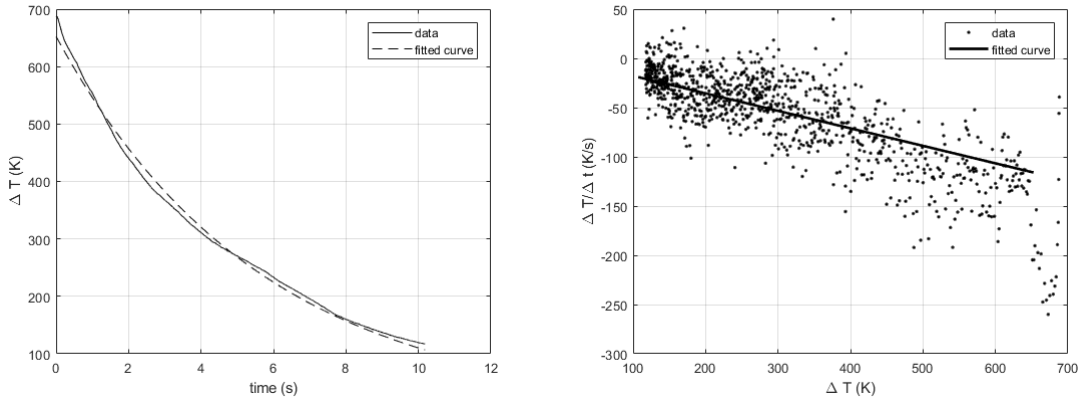

(a) Exponential fitted curve. **(b)** Derivative of the curves.

Figure 3.6: An exponential fit to Renovas preliminary temperature profile in Figure 3.5a using Equation 3.1. The temperature curve is referred to as data in the legend.

To achieve a temperature curve with the contribution from the flame included, like the curve in Figure 3.5b, it can be assumed that the impact from the flame is a constant release of heat for the time period which the gas flow exists inside the flame. This can be implemented as a constant source term which can then be combined with the fitted cooling rates from Figure 3.6b to obtain a more realistic temperature curve. The residence time of the gas in the flame was estimated from the CFD-model by finding the time it takes for the mean flow field to reach a certain height in the boiler which corresponds to the extinction of the flame.

The temperature curve was then calibrated so that the correct amount of heat was released from the flue gas. Additionally, the curve could be fitted to the correct outlet temperature by varying the intensity of the source term and the decay factor in Figure 3.6a. This resulted in a temperature curve with 30% higher cooling rate than the one in Figure 3.5a, which can probably be explained by the amount of precipitation on the boiler walls. More details regarding the heat source can be found in Appendix E.1.

The addition of the heat source term was implemented and calculated for all measured cases but for the sake of simplicity and robustness it was decided to find one curve that can be used to predict the degree of sulfation for all cases of the Renova boiler. This curve should preferably have a similar peak temperature as the MEC boiler and have an end temperature close to the mean end temperature of the nine measured cases. The case which curve fits these conditions best was the 8th and thus it was chosen to be used for all CHEMKIN simulations of the Renova boiler. It can be seen in Figure 3.7a below.

Since a thorough CFD-analysis with combustion has been conducted for the MEC boiler it was decided to use the curve in Figure 3.5b for the CHEMKIN simulations of the MEC-boiler. However, since the curve is spiky in some locations, which may affect the kinetics considerably, a smoothing of the curve was performed in

MATLAB which resulted in the curve shown in Figure 3.7b below. The smoothing was done by smearing out the data points with the largest deviations with their neighbouring data points and thus retain the same average in the interval.

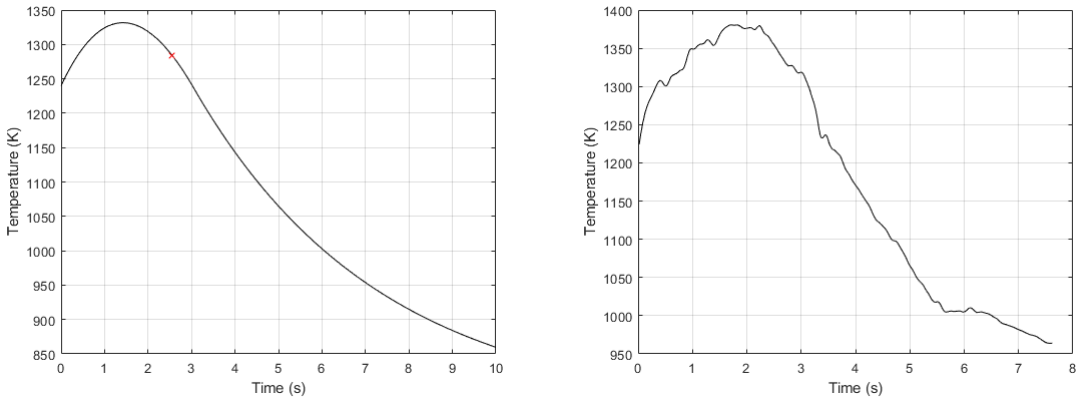

(a) Refined temperature curve for the 8:th measured case of the Renova boiler.

(b) Smoothed curve of the MEC-boiler.

Figure 3.7: Final temperature curves for both boilers.

3.4 Preparation for simulations in CHEMKIN

As mentioned earlier in this chapter; the flow rates, compositions and heat released from the Renova boiler were calculated using mass- and energy balances over the boiler and the flue gas aftertreatment system. This procedure was automated so that it could be used to calculate the initial conditions for each measured case of the Renova boiler. The initial conditions for the experimental cases of the MEC boiler were also calculated with a similar procedure but with a few additional assumptions due to less available data. This is further explained in Section 3.7. In addition, carbon monoxide was added in a way so that the environment in the boiler is more representative of the reality. This is due to the need of radicals which the oxidation of carbon monoxide generates. Since a heat source had already been created to represent the flame, it could also be used as a measure of the time that carbon monoxide should be more or less fully oxidized. In an ideal scenario, the carbon monoxide should be fully oxidized by the time the flame ends but the non ideality was accounted for with the parameter CO_{inj} which is described in Section 3.6.

The composition of the fly ash was measured in a previous experimental work as described in Section 1.3. This is the main source of information available, together with the stack concentrations gathered from Renova, for determination of the composition in the flue gas and inlet conditions for the simulations. Below, it will be described what assumptions were made in order to translate the information in the fly ash measurements into useful information for the simulations.

The total amount of potassium, sodium and calcium as well as sulfur and chlorine were measured in the fly ash and it is assumed that all potassium and sodium

exists as either chlorides or sulfates in the ash. The distribution of chlorine and sulfur is assumed to be the same for potassium and sodium. In addition to chlorides and sulfates, the calcium is also assumed to exist as calcium oxide and the fraction of calcium oxide is calculated as the excess of calcium so that the mole balance is fulfilled. The reasoning behind these assumptions is that it seems that most alkali is released as chlorides in the char combustion phase during combustion of biomass. This is not specific for MSW but should apply to it as well since the chlorine content is high [16]. The sulfation process will then decide how much of these chlorides that will become sulfates. For the calcium; it is reasonable that the majority is released as calcium oxide and that some is released as calcium sulfate. This is due to the fact that calcium chloride oxidizes fast at the high temperatures of the burning fuel (>1000K) [7]. It is very possible however that some calcium chloride exists in the ash, which the literature also suggests [17], it is however assumed here that these chlorides are produced after the sulfation process since calcium chloride is not stable at high temperatures.

Calcium and alkali are assumed to have the same chlorine per sulfur ratio in the fly ash. In reality, calcium behaves very differently from alkali in the course of interest. As opposed to potassium and sodium, which mainly exists as chlorides when they release from the fuel bed, calcium should mainly exist as oxides and sulfates. A comparison can be made for the amount of calcium per alkali and the total chlorine per sulfur ratio in the measured fly ash composition. It can be noted that there is a tendency that the chlorine per sulfur ratio is slightly higher for calcium than for the alkali since more calcium per alkali results in more chlorine per sulfur. This can be seen in Figure 3.8 below. The assumption that calcium has the same chlorine per sulfur ratio as alkali may not be correct but it is simple and robust since it can handle big differences in calcium and alkali concentration. Other assumptions that were tested, for example keeping the calcium chloride concentration at a constant percentage level between all tested cases, did not work as well in this regard.

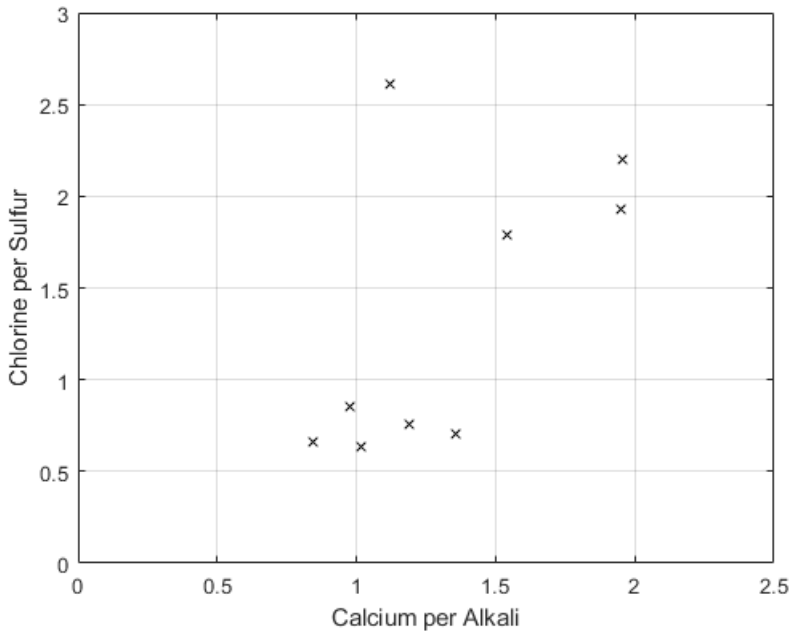

Figure 3.8: Calcium per alkali ratio plotted against chlorine per sulfur ratio to investigate the chlorine per sulfur ratio for calcium.

3.5 CHEMKIN setup

In this chapter, the CHEMKIN setup for the Renova boiler is presented. The differences between the Renova and MEC boilers regarding the setup and simulations is explained in 3.7. The setup for the Renova boiler in CHEMKIN consisted of; two plug flow reactors, main inlet, oxygen injection, carbon monoxide injection, sulfur dioxide injection as well as a mixer for the sulfur dioxide injection. The setup is shown in Figure 3.9 below. The inlet of the system was defined by the flow and composition of species that are released from the fuel bed while the outlet was the end of the boiler in Figure 3.3a.

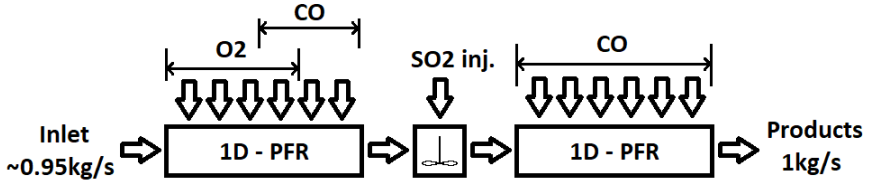

Figure 3.9: Setup of the simulation in CHEMKIN. The injections of oxygen and carbon monoxide are continuous over time while the injection of sulfur dioxide is instantaneous.

It was decided that two cases should be used for comparison in the CHEMKIN simulations, namely the 1st and the 8th case. The primary reason why these cases

were chosen was that the 8th case had an injection of sulfur dioxide and that the 1st case did not. Additionally, the two cases had very different conditions. Case 1 had a high concentration of sulfur dioxide at the inlet and a low amount of potassium chloride. Case 8, on the other hand, had opposite conditions which made these two interesting for comparison. Note that these two cases should not be compared to visualize the effect of the sulfur dioxide injection since they have very different inlet conditions.

3.5.1 Reactors

The plug flow reactors (PFR) were chosen because they can represent the pathline of a gas volume travelling through the boiler well. The reason why two reactors are needed is because of the injection of sulfur dioxide. The first reactor represents the boiler before the injection and the second reactor represents after the injection. With this method, the injection can be implemented instantaneously when the flow goes into the second reactor. Because of this, the temperature profiles had to be split in two parts; one part before injection and one part after injection. The time of injection was determined in the CFD-simulation by plotting the position in the vertical direction against time. The injection time is then the time at which the mean flow reaches the position of the injection nozzles.

Injections and residence time are both related to distance through the PFR. A direct relation between time and distance is therefore desirable and can be achieved using a constant axial velocity which can be implemented in several ways. The chosen method was to let the diameter of the reactors vary to make up for the change in volume flow due to change in temperature and molar amount. The reason why this is necessary is because the temperature profiles already accounts for velocity changes in the CFD-model since they are defined as temperature per residence time. Since the residence time will adjust itself by regulating the flow rate, the length was arbitrarily set to 10 m. Since the first reactor should have a smaller residence time, it means that it will also have a substantially smaller diameter so that the gas will flow through the reactor faster. The residence time for the first and second PFR was 2.55 and 7.53 seconds respectively.

3.5.2 Inlet conditions

The main inlet was defined with an arbitrary mass flow rate and the composition of the main flow can be found in Table 3.1. The sulfur dioxide that was included here is only the sulfur dioxide which originates from the fuel since the injection is implemented later. It is assumed that all potassium and sodium leaves the fuel, and thus enters the reactor, as chlorides. If the concentration of hydrochloric acid in the system would be low, the alkali chloride would instantaneously release its chloride to form hydrochloric acid. The calcium on the other hand is assumed to leave the fuel bed partly as calcium oxide and partly as calcium sulfate. The amount of calcium oxide is assumed to be constant throughout the whole boiler and is calculated as the excess after potassium, sodium and calcium have consumed all chlorine and sulfur

in the fly ash. To get a hint of how the calcium oxide behaves at high temperature, calculations of the conversion from calcium oxide to calcium sulfate were performed with the rate expressions proposed by Seehra and Gopalakrishnan [8]. According to the calculations, which are shown in Appendix E.2, the conversion is negligible for even the smallest of particle sizes in waste incineration fly ash measured by Sun et. al [18]. This motivates the choice to neglect the formation of new calcium sulfate in the boiler. Figure 3.10 below displays an example of how the distribution can look like with this assumption. The change from Figure 3.10a to Figure 3.10b demonstrates what happens with the alkali in the CHEMKIN simulation and from Figure 3.10b to Figure 3.10c what happens with the calcium after the simulation. The sulfur that is added in Figure 3.10b originates from the sulfur dioxide and the chloride leaves as hydrochloric acid.

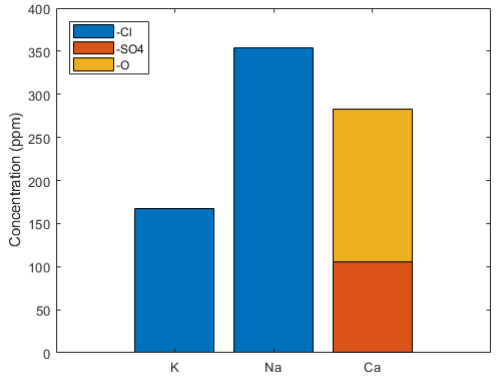

(a) Distribution when released from the fuel bed.

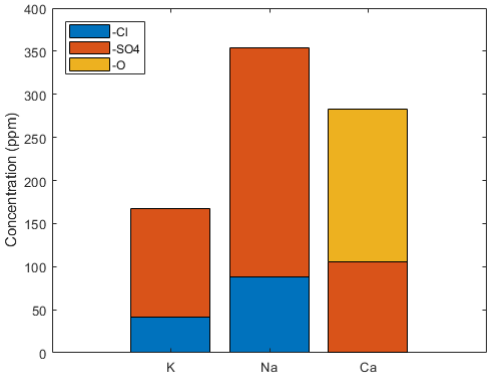

(b) Distribution after the CHEMKIN simulation.

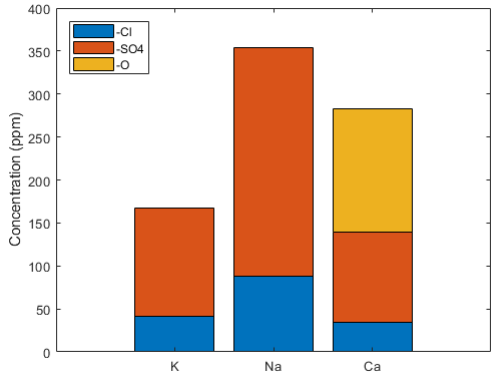

(c) Distribution in the fly ash.

Figure 3.10: An example of how the distribution of salts can change through the sulfation process for Potassium, Sodium and Calcium.

All calcium that does not leave the fuel bed as oxide is assumed to be calcium sulfate. The calcium chloride is assumed to be formed from the calcium oxide at lower temperatures, after the sulfation of the alkali. Its effect on the chloride concentration in the simulation is therefore neglected. Since the concentration of

neither calcium chloride nor calcium sulfate will change all calcium is assumed to be inert throughout the CHEMKIN simulation.
Potassium and sodium are assumed to behave identically in the sulfation process since sufficient data for sodium is not available. Therefore, the total amount of sodium is simply added to the total amount of potassium for the CHEMKIN simulations. The main motivations for this assumption is that potassium and sodium behave similarly and that the rate constants for potassium and sodium should depend on the concentration of the other.

The chlorine is assumed to leave the fuel bed as hydrochloric acid and potassium chloride (and therefore also sodium chloride). The hydrochloric acid is made up of the chlorine that is not bonded to the alkali. The total amount of chlorine is calculated by adding together the chloride in the fly ash and the hydrochloric acid in the flue gas leaving the boiler which in turn is calculated from the stack concentration of hydrochloric acid as well as the amount of chlorine removed in the scrubber. These assumptions should be fairly valid as long as there are no substantial amounts of other chlorine species, which there should not be.

Table 3.1: Main inlet properties for the CHEMKIN simulations of the Renova boiler with the reference model. The properties are shown for one case without sulfur injection (Case 1) and one case with sulfur injection (Case 8). In reality, H_2 and H_2S represents H_2O and SO_2 respectively.

Measured case	Case 1	Case 8
Inlet flow $[m3/s]$	0.9488	0.94976
N_2 [mole%]	71.93	70.44
H_2 [mole%]	16.93	18.67
CO [mole%]	11.03	10.80
H_2S [ppm]	237	149
KCl [ppm]	340	424
HCl [ppm]	471	370

3.5.3 Injections

If all oxygen, carbon monoxide, sulfur dioxide and alkali chlorides are implemented at the inlet for the simulations simultaneously; an extremely fast sulfation occurs during the first second where the carbon monoxide will oxidize completely in a few time steps. This is not realistic since the carbon monoxide in practice should not be fully oxidized until the peak temperature. The time of the peak temperature is referred to as t_f and will be discussed more further on.

In reality, the SO_2-injection consists of multiple sprays of sulfuric acid from the walls of the boiler. Sulfuric acid has been found to decompose to SO_3 which in turn reacts rapidly to SO_2 [19]. Unfortunately, since the CHEMKIN simulation is entirely in 1D and assumes 100 % mixing, implementing the injection as SO_3 leads to extremely high degrees of sulfations, therefore SO_2 is used in the simulations, following from the assumption that decomposition to SO_2 occurs more rapidly than

mixing. This injection is the only one that exists in reality and the theoretical injections of carbon monoxide and oxygen are simply there as an attempt to account for mixing.

In order to simulate more realistically; the oxygen is injected with time, adjusted so that most carbon dioxide has been formed by the time the flame ends. This ensures a more stretched out course of sulfation which is more realistic. After oxygen becomes abundant, a small amount of carbon monoxide was injected to account for radicals and bad mixing. When this method was tested, some of the water was converted into hydrogen- and oxygen gas which should not happen in reality. For this reason, the water was instead added as hydrogen gas and the total amount of injected oxygen was adjusted accordingly. The same was done with sulfur dioxide which enters the inlet in the form of hydrogen sulfide, although rapidly decomposes into radicals. A more detailed description of the injections can be found in Appendix E.1. The total amount of injected oxygen, carbon monoxide and sulfur dioxide are shown as proportions of the exiting flue gas in Table 3.2 below.

Table 3.2: Injections of oxygen, carbon monoxide and sulfur dioxide shown as proportions of the exiting flue gas.

Measured case	Case 1	Case 8
$O_{2,inj,tot}$ [mole%]	18.57	19.19
$CO_{inj,tot}$ [mole%]	0.1054	0.1033
$SO_{2,inj}$ [ppm]	0	295

The design of the injections is illustrated in Figure 3.11a below. The inlet flow was scaled so that 1 kg/s was the resulting outlet flow where all concentrations are known. Figure 3.11b shows how the concentrations change when injections are used with the carbon monoxide injection barely being visible. Note that both hydrogen and carbon monoxide are fully consumed by the time oxygen becomes abundant after which the oxygen injection will dilute the system slightly.

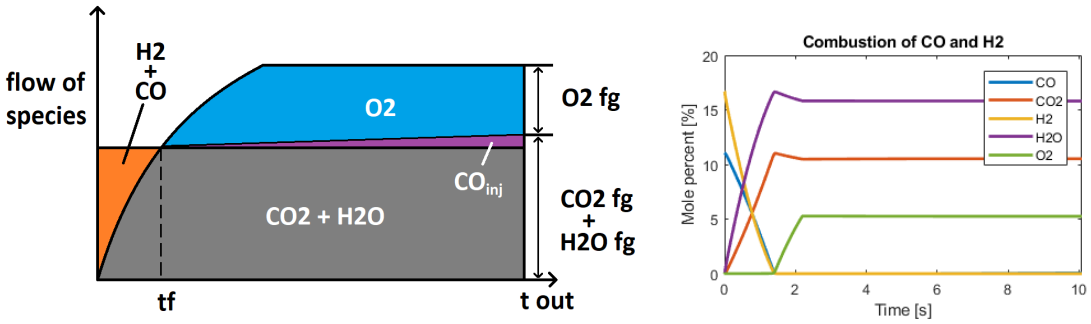

(a) Design of the injections.

(b) Molar concentrations of the involved species.

Figure 3.11: The development of species in the CHEMKIN-simulations.

The concentration of carbon dioxide at the outlet of the boiler has been calculated from the measured stack concentrations. In order for the carbon monoxide to oxidize gradually through the flame; the oxygen was injected gradually with time. This injection was customized so that all available carbon monoxide has been consumed by the time the flame has ended. The point where oxygen becomes abundant and all the fuel is consumed defines the highest temperature in the flame. The time of this point is referred to as t_f in Figure 3.11 and is equal to 1.4 seconds in the reference model.

It is however also desirable to have a small effect from the oxidation of carbon monoxide throughout the entire boiler because in reality all carbon monoxide will not be consumed in the flame due to incomplete mixing. This was implemented with the carbon monoxide injection from the point where the flame ends to the outlet. The amount of carbon monoxide to be injected in this way is unclear but it is reasonable to assume that not more than 1000 ppm of the exiting flue gas would be realistic.

3.6 Simulation procedure

For the simulations in CHEMKIN, some assumptions were made in the form of parameters. This was done for the assumptions which have a wide range of possibilities. Two models with different sets of assumptions were simulated; one with theoretically reasonable parameter values called the reference model and one with values providing a good fit between the simulated and experimental results called the optimized model. It is of crucial importance to note that the assumptions made to reach the setup with the best fit does not reflect the reality. There are too many uncertainties in several of the assumptions to conclude that this combination is most realistic. However, together with the sensitivity analysis it may give some indications to which assumptions are most viable.

The parameters that were established to quantify the assumptions are shown in Equation 3.2-3.5 below.

$$X_S = \frac{x_{S,in}}{x_{S,ideal}} = \frac{\text{Amount of sulfur available from fuel}}{\text{Total amount of sulfur released from fuel}} \tag{3.2}$$

Equation 3.2 shows the chosen definition for the mixing parameter for sulfur. It is defined so that with ideal mixing it should be equal to 1 since then the mean content of sulfur is available for contact with all the other species. In the reference model it was equal to 1 but was allowed to be reduced for the optimized model.

$$X_{Cl} = \frac{x_{Cl,in}}{x_{Cl,ideal}} = \frac{\text{Amount of chlorine available from fuel}}{\text{Total amount of chlorine released from fuel}} \tag{3.3}$$

Equation 3.3 shows the chosen definition for the mixing parameter for chlorine. It is defined in the exact same way as for the sulfur in Equation 3.2 but with chlorine

instead. In the reference model it was equal to 1 but was allowed to be reduced for the optimized model.

$$X_{CaSO4,in} = \frac{\text{Amount of calcium sulfate released from the fuel}}{\text{Amount of calcium sulfate in the fly ash}} \tag{3.4}$$

Equation 3.4 shows the chosen definition of how much of the calcium sulfate in the fly ash that releases directly from the fuel. When this parameter is equal to 1; then it is assumed that all calcium sulfate releases from the fuel as calcium sulfate and is inert through the sulfation process. This also means that the sulfur contained in the calcium sulfate is not available for sulfation of potassium or sodium. In the reference model it was equal to 1 but was allowed to be reduced for the optimized model.

$$CO_{inj} = \frac{\text{Amount of carbon monoxide injected after flame}}{\text{Total amount of carbon monoxide}} \tag{3.5}$$

Equation 3.5 shows the chosen definition of the amount of carbon monoxide to inject after the flame. The main reason why some carbon monoxide was injected after the flame is that it otherwise would be completely oxidized before the flame has ended. This is because the carbon monoxide reacts so fast in CHEMKIN due to ideal mixing. The parameter enables the assumption of non complete combustion of carbon monoxide in the flame. In the reference model it was set to 1 % which corresponds to a combustion of 99 % carbon monoxide in the flame. This results in a total injection of about 1000 ppm carbon monoxide which was deemed fairly plausible. In the optimization it was allowed to vary but a significantly higher value is not very realistic.

The methodology used for the simulations was to first simulate the reference model for all experimental cases for both boilers. The set of assumptions for the reference model is shown in Table 3.3 below.

Table 3.3: Parameters used in the reference model.

Parameter	Value
X_S	100 %
X_{Cl}	100 %
$X_{CaSO4,in}$	100 %
CO_{inj}	1 %
t_f	1.4 s

After this, an optimization was performed where the assumptions were changed one by one in order to find out if a better fit to the measured degree of sulfation can be found. The general procedure was to iterate by "Trial and Error" but it was decided that only the most uncertain assumptions should be changed. These were shown in Equation 3.2-3.5. The parameters that were used in the optimized model is shown in Table 3.4 below.

Table 3.4: Parameters used in the optimized model.

Parameter	Value
X_S	33 %
X_{Cl}	50 %
$X_{CaSO4,in}$	50 %
CO_{inj}	3.25 %
t_f	1.4 s

3.7 Additional assumptions for the boiler at MEC

The available data from the sulfation measurements at MEC was not as extensive as the data from the experiments at Renova. Specific stack concentrations for each trial were not available so yearly averages were used instead. This means that eventual discrepancies in the concentrations of oxygen, carbon dioxide, water and hydrochloric acid are not accounted for. Since the MEC boiler has very similar components as the Renova boiler, it was assumed that the relative change in composition between the boiler outlet and the stack is the same for both boilers. This assumption could be used to determine the initial conditions for the simulations of the MEC boiler.

Another lack of data for the MEC-boiler was the amount of injected sulfur dioxide. Out of the six measurements; three were done without an injection which makes it possible to calculate the amount of sulfur released from the fuel. This was done because the sulfur content in the ash and the flue gas leaving the boiler is known. Therefore, an average sulfur content in the fuel had to be calculated based on these three measurements and then used in the simulations with sulfur dioxide injection.

The CHEMKIN setup for the MEC boiler differs slightly from the Renova boiler. The main difference is that the SO_2-injection is implemented at the inlet rather than after 2.55 seconds. This means that the CHEMKIN setup for the MEC boiler is the same as the setup shown in Figure 3.9 except that it consists of one continuous PFR of 7.62 seconds without a mixer for the SO_2-injection.

4

Results

In this chapter the results will be presented and discussed. Firstly, the comparison between experimental- and simulated results for the reference model will be shown. Then the results for the optimized model is presented. Additionally, the sensitivity analysis as well as discussion regarding the reaction rate and equilibrium will be featured here.

4.1 Reference model

The results from the simulations of the reference model is shown in this section. Figure 4.1 below shows the results for the Renova boiler and Figure 4.2 shows the results for the MEC boiler. 4.1a and 4.2a shows the degree of sulfation both from the simulation and experimental measurements, for each measured case. 4.1b and 4.2b shows the same results but plotted against amount of sulfur dioxide in the flue gas. It can be seen that the amount of available sulfur dioxide has a positive effect on the degree of sulfation.

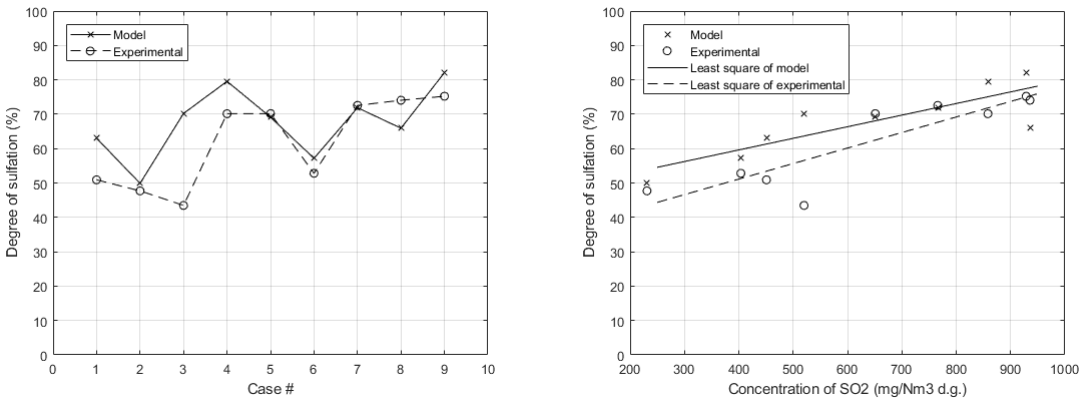

(a) Degree of sulfation for each experimental case.

(b) Degree of sulfation plotted against sulfur dioxide concentration.

Figure 4.1: Simulated and measured degree of sulfation for the Renova boiler.

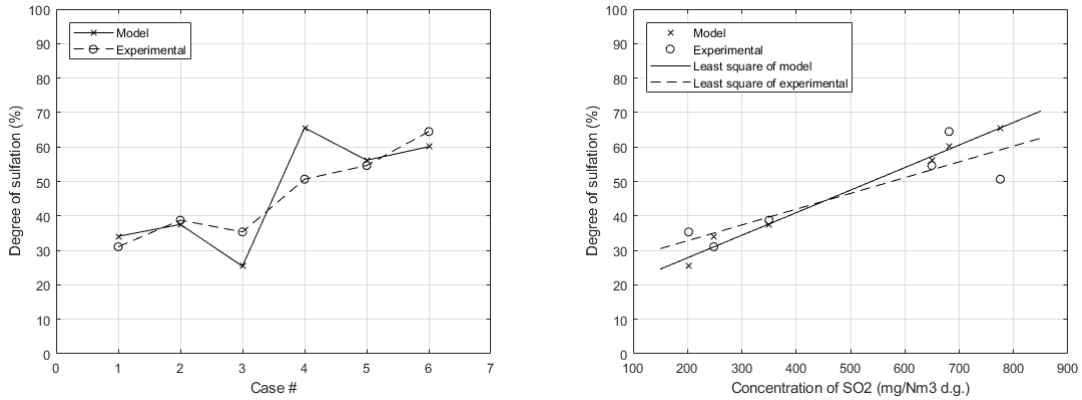

(a) Degree of sulfation for each experimental case.

(b) Degree of sulfation plotted against sulfur dioxide concentration.

Figure 4.2: Simulated and measured degree of sulfation for the MEC boiler.

It can be seen in Figure 4.1 that the degree of sulfation is considerably higher for the simulated- than for the measured values. The difference is even more pronounced for the first three cases, which are the cases without an injection of sulfur dioxide. However, in Figure 4.2 it can be seen that for the MEC boiler the fit is good between the simulated- and measured values.

When investigating how the degree of sulfation depend on the sulfur dioxide concentration, i.e. Figure 4.1b and 4.2b, it is noted that the slope of the least square approximation for the simulations of the Renova boiler is slightly lower than for the measurements. This suggests that dependency on the sulfur dioxide concentration is lower than it should be which is an expected result since sulfur dioxide is injected instead of sulfuric acid. For the MEC boiler however, the opposite can be said since the slope is higher for the simulated results than for the measurements. The reason that the MEC boiler has steeper slopes than the Renova boiler may very well be that the injection of sulfur dioxide is assumed to be at the inlet. Due to mixing, this may not be the case in reality and should probably have a delay before it reaches the mean flow path. One potential solution for this problem is the introduction of sulfur trioxide as part of the injection which would increase the degree of sulfation in the Renova model and not in the MEC model. This alternative will be discussed further in Section 4.5.10.

4.2 Optimized Renova model

In this section; the results for the optimized model for the Renova boiler is shown. Figure 4.3 below shows the results for the Renova boiler and as can be seen; the fit is very good between experimental data and simulations. Using the same setup for the MEC boiler resulted in very extreme degrees of sulfation for the cases with injection. While an optimization was attempted on the MEC boiler, the reference model was already more suitable than any optimized setup.

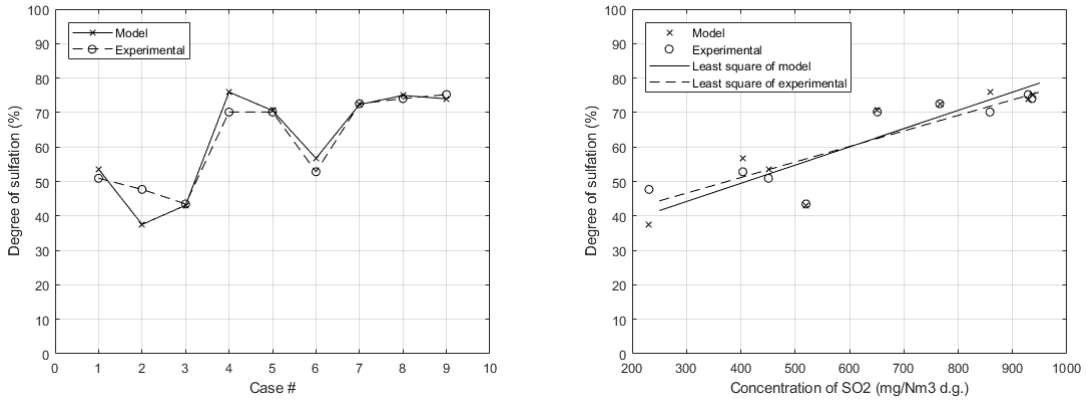

(a) Degree of sulfation for each experimental case.

(b) Degree of sulfation plotted against sulfur dioxide concentration.

Figure 4.3: Simulated and measured degree of sulfation for the Renova boiler.

4.3 Equilibrium vs. reaction rate

The equilibrium curve for potassium sulfate together with two scaled sulfation rate curves is shown in Figure 4.4 below. This Figure shows the importance of having a long residence time in a certain temperature interval. Not only does the temperature affect the rate at which sulfation takes place but also the equilibrium, i.e. the maximum allowed potassium sulfate at a certain temperature. Both the sulfation rate and the equilibrium are based on the final reaction where potassium sulfate is condensed. In reality, there are many reactions included so Figure 4.4 serves more as an indicator than a representation of the sulfation. The method used to produce the data for Figure 4.4 is by going from 1800 K to 1000 K in 10 seconds using reference case 8 with an excess of 5% oxygen. The results indicates that hydrochloric acid plays a big role in the initiation of the reaction at higher temperatures where the equilibrium between potassium hydroxide and potassium chloride occurs. A lower total concentration of chlorine drives the equilibrium to favor hydrochloric acid and potassium hydroxide which in turn reacts more aggressively than its counterpart.

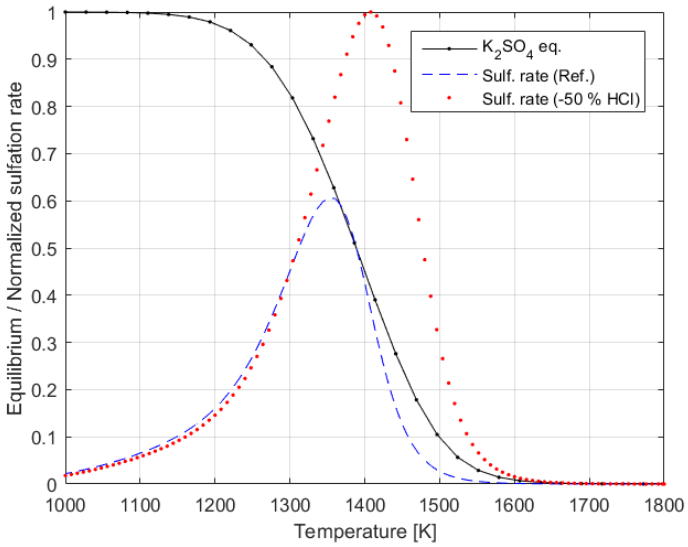

Figure 4.4: Equilibrium and relative sulfation rate. The reaction rates are for the formation of K_2SO_4 and are scaled to fit with the equilibrium curve.

4.4 Speciation

The following results show the course of the reactions for potassium, sulfur and chlorine. The paths that these atoms take from inlet to outlet is crucial for the understanding of the mechanisms. The form of which these species exist in during the course of the sulfation can be seen in Figures 4.5-4.7. In the figures, the concentrations of the molecules are scaled with the number of the relevant atoms they contain, i.e. for potassium, one K_2SO_4 molecule counts twice while one KCl molecule counts once. A few intermediates exist in lower concentrations and are therefore not displayed in the image. K_2SO_4(B) represents the condensed form of K_2SO_4 and K_2CL_2 the condensed form of KCl.

4.4.1 Potassium

In Figure 4.5 below, it can be seen that the majority of the potassium at any given time is either in the form of potassium chloride or potassium sulfate. The alternative species visible are some of the intermediates in the reaction, which are important. There are many intermediates that play a crucial role for the formation of potassium sulfate, such as radical potassium (K) and potassium bisulfate ($KHSO_4$), one of which is visible in Figure 4.5. Even K_2SO_4 in the gas phase condenses so rapidly that the gas phase concentration is negligible.

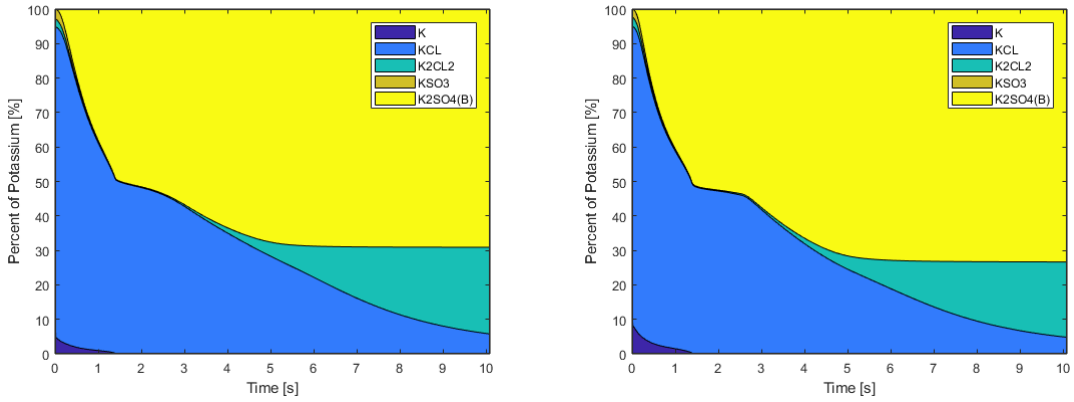

(a) Without SO_2-injection (Case 1). **(b)** With SO_2-injection (Case 8).

Figure 4.5: Potassium speciation through the Renova boiler with the reference model.

4.4.2 Sulfur

As can be seen in Figure 4.6 below, sulfur takes many different forms in the oxygen free environment. Most common are disulfur (S_2) and sulfur monoxide (SO) along with a few radicals. As soon as oxygen becomes abundant, sulfur exists only in the forms of sulfur dioxide and potassium sulfate, along with a small amount of sulfur trioxide. It can clearly be observed that even in the case where there is no SO_2-injection there is a lot of sulfur available for reaction. This indicates that factors other than the sulfur concentration can affect the sulfation process such as temperature, time and radicals.

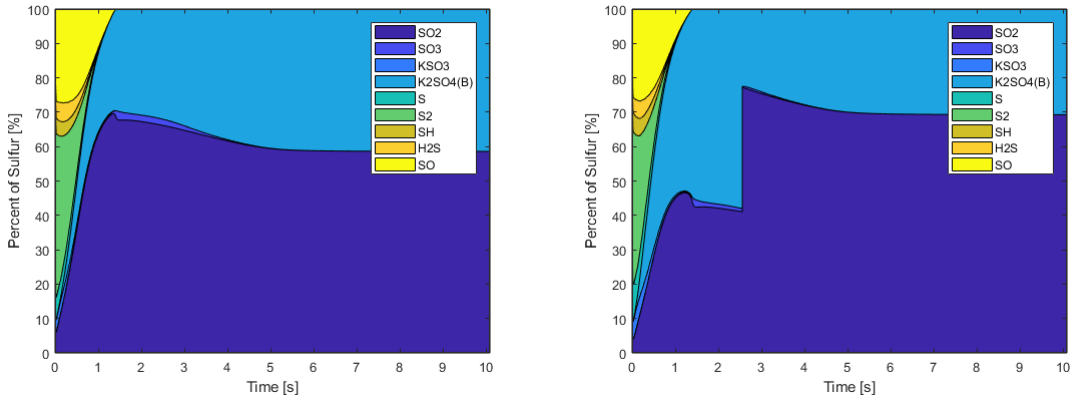

(a) Without SO_2-injection (Case 1). **(b)** With SO_2-injection (Case 8).

Figure 4.6: Sulfur speciation through the Renova boiler with the reference model. In the case with SO_2-injection, the total sulfur actually increases after the injection, all in the form of SO_2.

4.4.3 Chlorine

As can be seen in Figure 4.7 below, hydrochloric acid and potassium chloride are the only significant species that include chlorine. Hydrochloric acid and potassium chloride are very connected when the chloride in the system becomes limited. One reaction forms hydrochloric acid and elementary potassium from potassium chloride and water if there is a limited amount of chlorine. This reaction is strongly controlled by equilibrium and rapidly consumes or produces elementary potassium depending on the gas concentration of hydrochloric acid. The formed elementary potassium forms potassium sulfate more rapidly than potassium chloride. This implies that the presence of hydrochloric acid reduces the rate of sulfation.

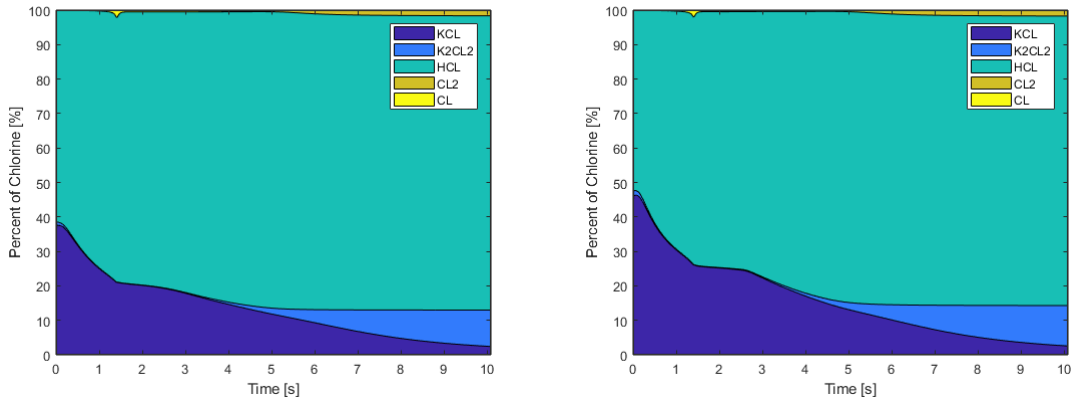

(a) Without SO_2-injection (Case 1 Renova).

(b) With SO_2-injection (Case 8 Renova).

Figure 4.7: Chlorine speciation through the Renova boiler with the reference model.

4.5 Sensitivity analysis

To investigate the impact that conditions and parameters had on the simulation, the parameters were varied with the reference model as a reference point for comparison. The resulting degrees of sulfation can be seen in the figures in this section. Analyses for MEC are only presented where it is believed to be relevant. A summary of the sensitivity analysis is shown at the end in Table 4.1.

4.5.1 Impact of hydrochloric acid

In Figure 4.8 below it becomes apparent that a lower concentration of hydrochloric acid released from the waste leads to a higher degree of sulfation. This is most likely since some of the potassium chloride reacts to hydrochloric acid and elementary potassium which is far less stable than potassium chloride, effectively increasing the rate of sulfation. This occurs especially in the first half second of the simulation and does not significantly affect the influence of the SO_2-injection. These results agrees well with the results shown in Section 4.3.

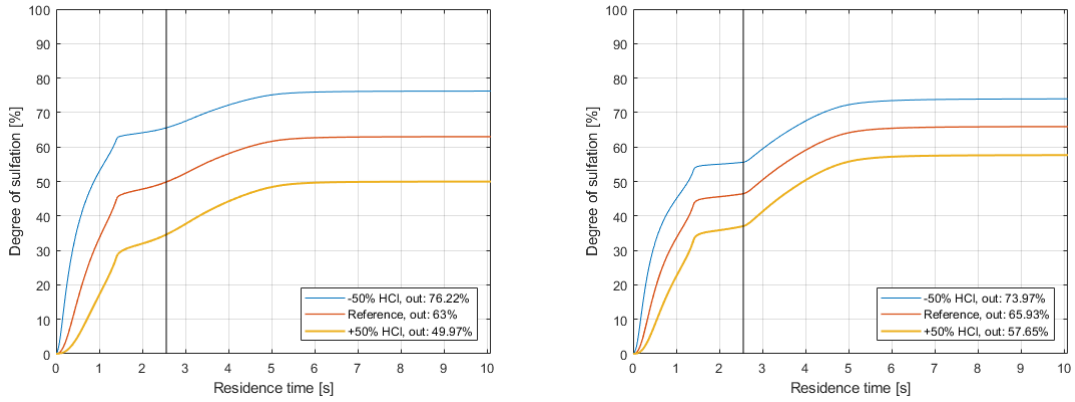

(a) Without injection (Case 1 Renova). **(b)** With injection (Case 8 Renova).

Figure 4.8: Simulated degree of sulfation for different concentrations of hydrochloric acid, with and without injection.

4.5.2 Impact of water

As seen in Figure 4.9 below, an increase of the water content initially increases the sulfation rate in the system but later reduces it. The reason for this increase is that water enters the system in the inlet in the form of hydrogen gas which then gets oxidized into water, as mentioned in Section 3.5. One possible explanation for the negative effect on the sulfation is that despite that radicals such as H increase the rate of sulfation, the presence of water reduces it, most likely by acting a buffer for radicals.

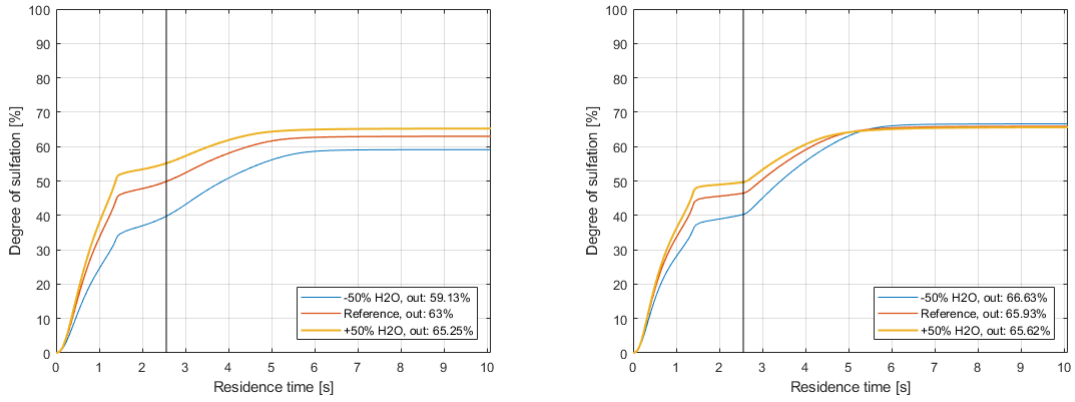

(a) Without injection (Case 1 Renova). **(b)** With injection (Case 8 Renova).

Figure 4.9: Simulated degree of sulfation for different concentrations of water, with and without injection.

4.5.3 Impact of carbon monoxide injection

As can be seen in Figure 4.10 below, higher carbon monoxide injections leads to higher degrees of sulfation. Since it increases the sulfation after the flame CO_{inj}

increases the influence of the SO_2-injection. The reason to why it increases the rate of sulfation is that the combustion produces a pool of radicals which is consumed by the sulfation process, especially radical oxygen. Even a relatively small pool of radicals boosts the sulfation rate drastically.

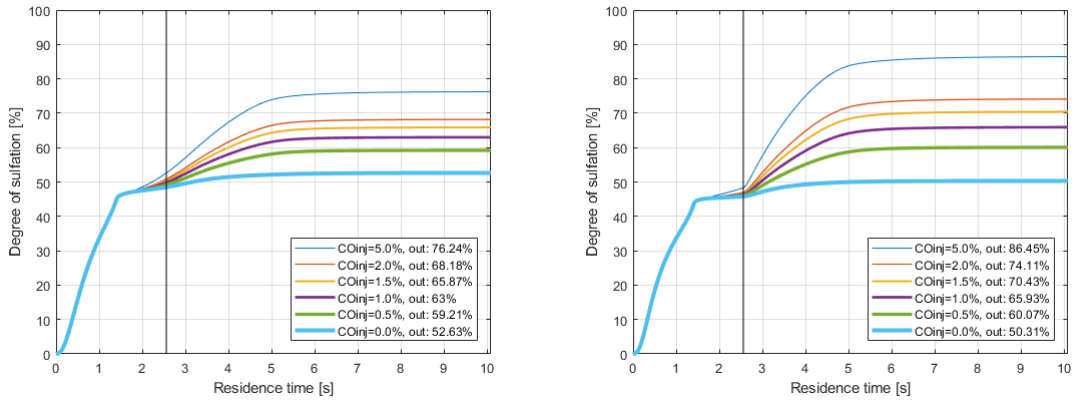

(a) Without injection (Case 1 Renova). **(b)** With injection (Case 8 Renova).

Figure 4.10: Simulated degree of sulfation for different values for the parameter CO_{inj}, with and without injection.

4.5.4 Impact of X_{Cl}

Figure 4.11 below shows the impact when changing the amount of chlorine in the fuel. Because of the definition mentioned in Equation 3.3, a low value for X_{Cl} can result in less chlorine than expected potassium chloride. If this occurs then reducing the concentration of hydrochloric acid is not enough; potassium chloride also needs to change form. For the sake of simplicity, the alternative form was set to potassium hydroxide which instantly reacts to form elementary potassium along with some intermediates. Some of this elementary potassium lasts all the way to the outlet without being sulfated. As mentioned earlier, the reason to why a lower X_{Cl}, i.e. a lower chlorine concentration, leads to higher degree of sulfation is because elementary potassium is less stable than potassium chloride and forms potassium sulfate quicker than potassium chloride does. This is true also when the chlorine concentration surpasses the potassium concentration.

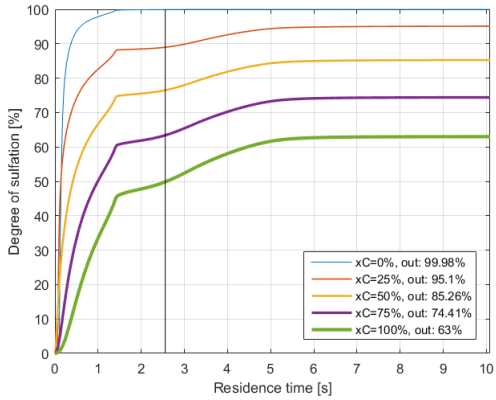

(a) Without injection (Case 1 Renova).

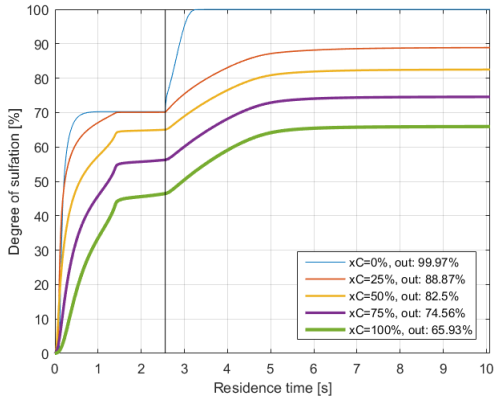

(b) With injection (Case 8 Renova).

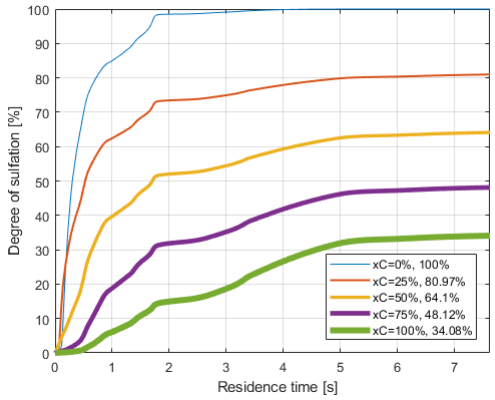

(c) Without injection (Case 1 MEC).

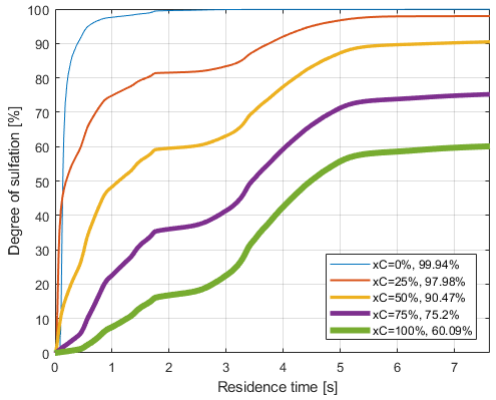

(d) With injection (Case 6 MEC).

Figure 4.11: Simulated degree of sulfation for different values for the parameter X_{Cl}, with and without injection.

4.5.5 Impact of X_S

For obvious reasons, a decreased amount of sulfur leads to decreased sulfation. This can be observed in Figure 4.12 below. As seen in Figure 4.6, only approximately half of the sulfur dioxide is consumed to produce potassium sulfate in the case without SO_2-injection. This means that even if there is an excess of sulfur in relation to potassium, the main driving force of the sulfation, i.e. sulfur concentration can still increase.

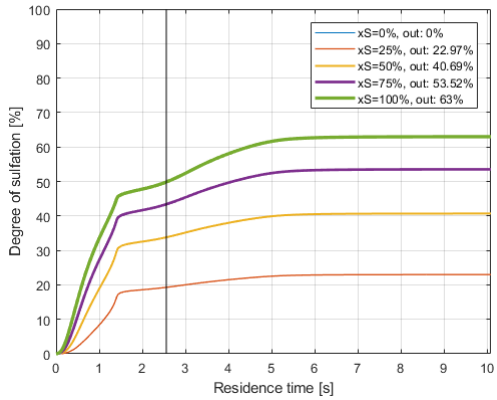

(a) Without injection (Case 1 Renova).

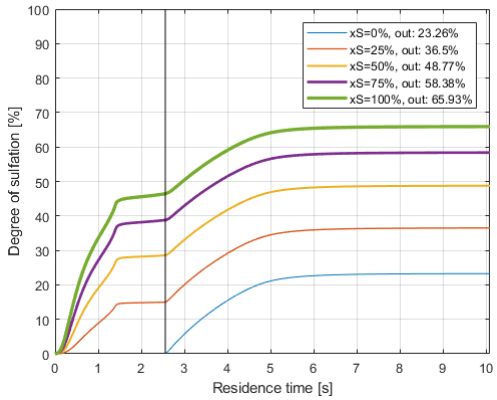

(b) With injection (Case 8 Renova).

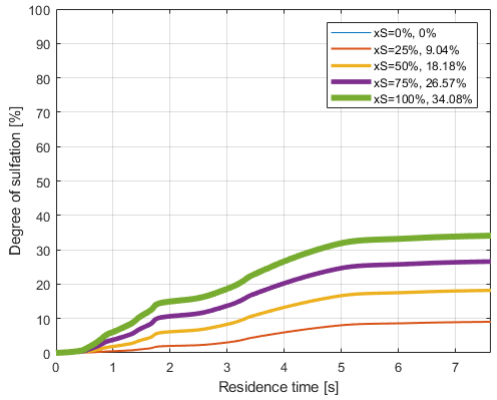

(c) Without injection (Case 1 MEC).

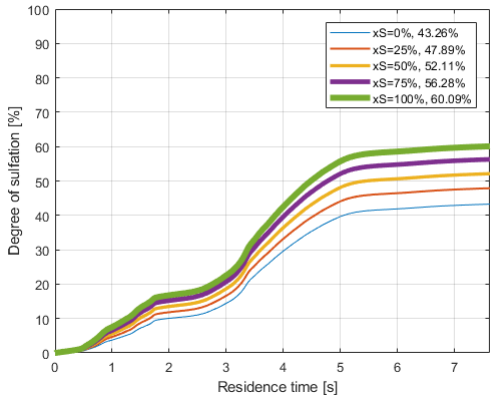

(d) With injection (Case 6 MEC).

Figure 4.12: Simulated degree of sulfation for different values for the parameter X_S, with and without injection.

4.5.6 Impact of $X_{CaSO4,in}$

The parameter $X_{CaSO4,in}$ does not differ much from the parameter X_S since they both only affect the sulfur concentration at the inlet. Unlike X_S however, higher $X_{CaSO4,in}$ lead to a lower concentration of sulfur rather than the opposite. This is because of the definition of $X_{CaSO4,in}$ which can be found in 3.6 where $X_{CaSO4,in}$ is the proportion of the expected calcium sulfate at the outlet that is expected to already have formed before the inlet. With this said, $X_{CaSO4,in}$ will decrease the sulfur depending on the amount of calcium in the system along with the expected sulfation rate. The results can be seen in Figure 4.13 below.

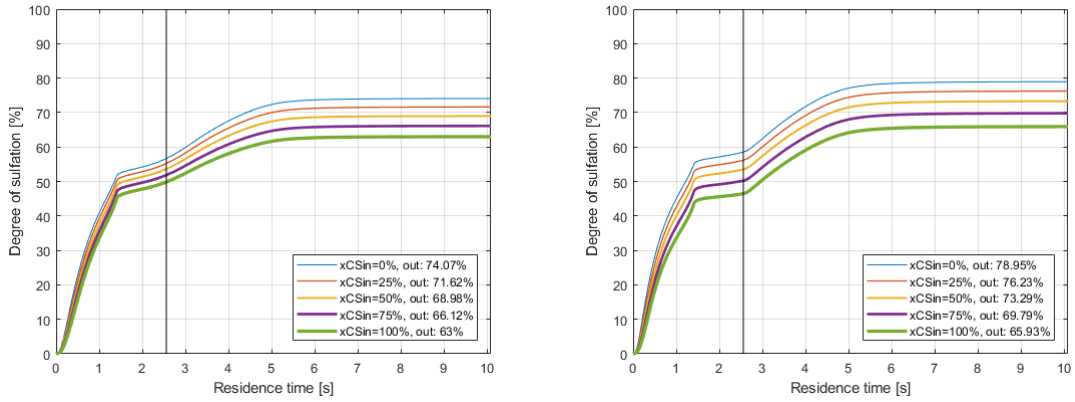

(a) Without injection (Case 1 Renova). **(b)** With injection (Case 8 Renova).

Figure 4.13: Simulated degree of sulfation for different values for the parameter $X_{CaSO4,in}$, with and without injection.

4.5.7 Impact of flame time, t_f

The flame time, t_f, is defined as the time of the peak temperature. In this sensitivity analysis however, t_f is changed after the temperature curve is produced which means that a change in t_f only impacts the setup for CHEMKIN, primarily the point where oxygen becomes abundant. This is done to solely investigate the kinetic impact of the flame time without bringing other effect into account. As can be seen in Figure 4.14, the value of t_f appears to completely change the nature of the simulation. The sulfation rate seems to get affected both by the compositions due to the change in t_f but also by the temperatures at time t_f. With the reference model, both a high and low t_f appears to result in high degrees of sultfation. Since the circumstances are changed by this value it is uncertain what the result would be when using a different setup of parameters, other than that of the reference model.

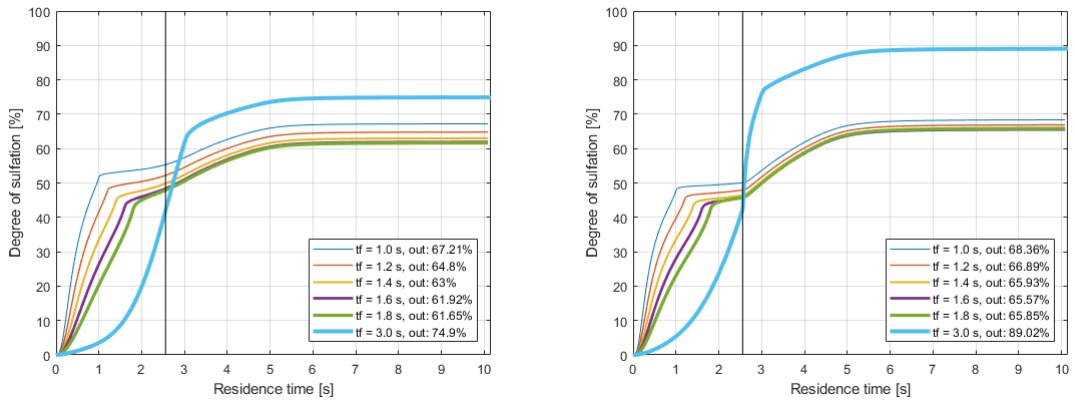

(a) Without injection (Case 1 Renova). **(b)** With injection (Case 8 Renova).

Figure 4.14: Simulated degree of sulfation for different values for the parameter t_f, with and without injection.

4.5.8 Impact of peak temperature, T_{peak}

To investigate how the temperature influences the reaction the intensity of the heat source term described in Appendix E.1 was adjusted. To compensate for this the factor for the cooling rate was adjusted to reach the correct outlet temperature. Note that because the sum of the heat source changed, the energy balance is no longer fulfilled. As can be seen in Figure 4.15 below, Temperature appears to greatly affect the sulfation rate. Sulfation of potassium primarily occurs in a certain temperature interval, which means that longer residence times within this interval will increase the degree of sulfation. A higher peak temperature will thus pass this interval quicker resulting in lower degree of sulfation. Judging from Figure 4.15, it would appear that the decreased peak temperatures are more beneficial for the reaction up until the peak. After the peak, i.e. after t_f the kinetics seem to be limited more to the equilibrium, which is why the sulfation rate is low for the curve with decreased peak temperature and significant for the curve with increased peak temperature.

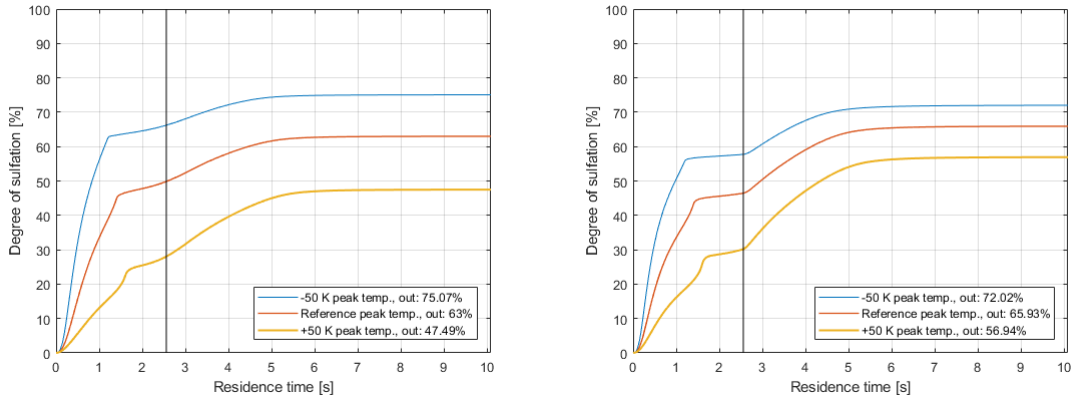

(a) Without injection (Case 1 Renova). **(b)** With injection (Case 8 Renova).

Figure 4.15: Simulated degree of sulfation for different temperature curves with varying temperature at the peak, with and without injection. The inlet and outlet temperature remain the same.

4.5.9 Impact of cooling rate

To investigate the influence that the cooling rate has on the sulfation the outlet temperature was varied with 50 K around the reference for Renova. The given temperature curve for MEC was not controllable and the cooling rate could not be changed. Therefore, the time vector of the temperature curve was scaled by a factor thus reducing or increasing the time at each time step. The oxygen injection is not scaled which is why the leap at 1.7 seconds is the same for all MEC curves. Important to note is that both of these methods affect the cooling rate but not necessarily equally much. As can be observed in Figure 4.16 below the degree of sulfation increases with a slower cooling rate. This is an expected result since a slower cooling rate gives a longer residence time in the temperature interval where the sulfation reactions occur. This is especially apparent since the curves are more

or less identical until the point where they one at a time flatten out since they reach the temperature at which sulfation no longer occurs.

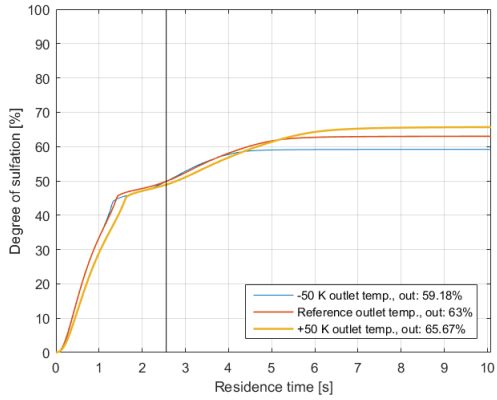

(a) Without injection (Case 1 Renova).

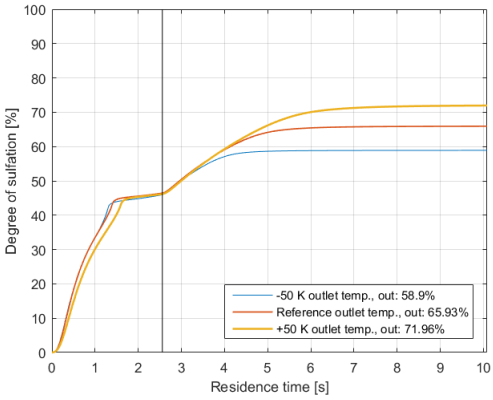

(b) With injection (Case 8 Renova).

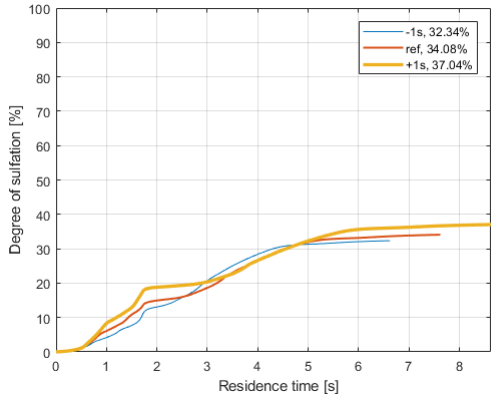

(c) Without injection (Case 1 MEC).

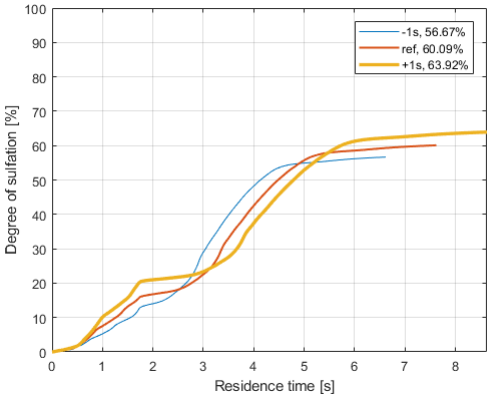

(d) With injection (Case 6 MEC).

Figure 4.16: Simulated degree of sulfation for different temperature curves with varying cooling rate with and without injection. The Renova boiler has its cooling rate increased by adjusting the outlet temperature while MECs cooling rate is adjusted by scaling the residence time.

4.5.10 Impact of SO_3-injection

Both the reference- and optimized model contained injections of pure SO_2. In reality the injection in the boilers consist of H_2SO_4 which decomposes to SO_3 at high temperatures which in turn also breaks down to SO_2 [19]. This intermediate SO_3 was found react more aggressively thus increasing the sulfation. In Figure 4.17a It is clearly visible that SO_3 increases the sulfation but only half a second later the rate of sulfation is once again the same for all the simulations. This big leap in just one or two times steps after the injection enters implies that the effects of the injection is unrealistically quick. This is because the effects of mixing is not accounted which is the one reason why partially injecting SO_3 instantaneously cannot be used as a substitute for injecting H_2SO_4 in the simulations. Despite the big leap and everything being assumed to be fully mixed not all of the SO_3 produces

K_2SO_4. In the simulation with 25% SO_3 in the injection only 65.6 % of the SO_3 contributes to the production of K_2SO_4 while the rest is reduced to SO_2 (70.25 ppm SO_3 lead to 46.06 ppm extra K_2SO_4). In Figure 4.17b it is visible that the oxygen free environments reduces the SO_3 (and SO_2) before any sulfation can occur, assuming that the injection occurs at zero seconds.

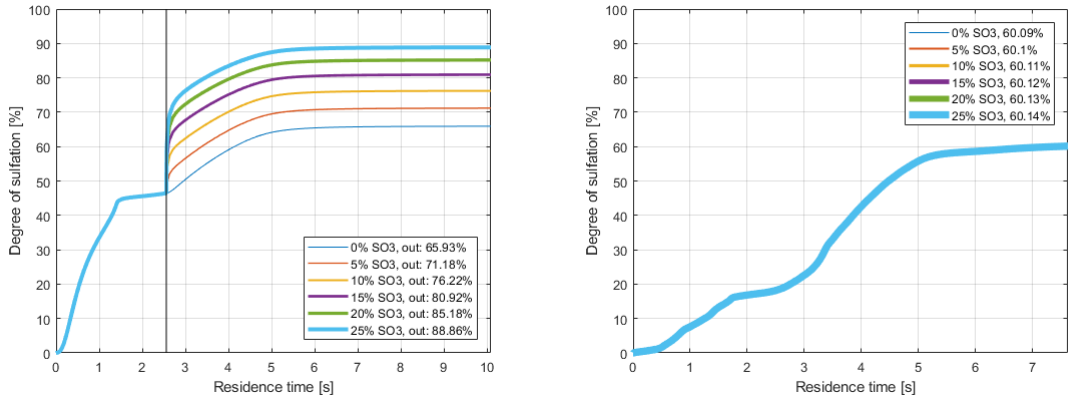

(a) With injection (Case 8 Renova). **(b)** With injection (Case 6 MEC).

Figure 4.17: Simulated degree of sulfation for different concentrations of SO_3 in the injection, for Renova and MEC.

The impact from SO_3 is interesting since it has a great potential of increasing the degree of sulfation. This could very likely be the missing link explaining why the reference model fits badly for the Renova boiler but much better for the MEC boiler. Implementing some of the injection as SO_3 increases the impact of sulfation for the Renova boiler but not the MEC boiler. The alternative, which is to increase the carbon monoxide injection, is not only unreasonable but also results in extreme degrees of sulfation for the MEC boiler.

4.5.11 Summary of the sensitivity analysis

Table 4.1 below shows a summary of the sensitivity analysis. This table gives an understanding of which parameters and conditions that affect the degree of sulfation. Sulfur increases the sulfation rate while chlorine suppresses it. Carbon monoxide added after oxygen becomes abundant increases the the sulfation rate, especially if additional SO_2 is injected. High residence time in the temperature range between 1100 and 1300 K also seems to be favorable for the sulfation process. SO_3, if it exists, would increase the sulfation, at least according to the used kinetic model. Water is important for the start of the reaction but seems to even out. Lastly, hydrochloric acid seems to be of special importance in the beginning, most likely since a chlorine deficiency breaks down potassium chloride into elementary potassium which is less stable than potassium chloride and increases the rate of sulfation.

Table 4.1: The results of the sensitivity analysis. ^{M} indicates the results are based on the MEC boiler.

Parameter	Low	Medium	High
HCl	-50 %	Ref.	+50 %
Sulf.	76.22 %	63.00 %	49.97 %
Sulf. (inj)	73.97 %	65.93 %	57.65 %
H_2O	-50 %	Ref.	+50 %
Sulf.	59.13 %	63.00 %	65.25 %
Sulf. (inj)	66.63 %	65.93 %	65.62 %
CO_{inj}	0.5 %	1 % (Ref.)	1.5 %
Sulf.	59.21 %	63.00 %	65.87 %
Sulf. (inj)	60.07 %	65.93 %	70.43 %
X_{Cl}	50 %	75 %	100 % (Ref.)
Sulf.	85.26 %	74.41 %	63.00 %
Sulf. (inj)	82.50 %	74.56 %	65.93 %
Sulf.^{M}	64.10 %	48.12 %	34.08 %
Sulf. (inj)^{M}	90.47 %	75.20 %	60.09 %
X_S	50 %	75 %	100 % (Ref.)
Sulf.	40.69 %	53.52 %	63.00 %
Sulf. (inj)	48.77 %	58.38 %	65.93 %
Sulf.^{M}	18.18 %	26.57 %	34.08 %
Sulf. (inj)^{M}	52.11 %	56.28 %	60.09 %
$X_{CaSO4,in}$	50%	75%	100 % (Ref.)
Sulf.	68.69 %	66.12 %	63.00 %
Sulf. (inj)	73.29 %	69.79 %	65.93 %
t_f	1.0 s	1.4 s (Ref.)	3.0 s
Sulf.	67.21 %	63.00 %	74.90 %
Sulf. (inj)	68.36 %	65.93 %	89.02 %
T_{peak}	-50 K	Ref.	+50 K
Sulf.	75.07 %	63 %	47.49 %
Sulf. (inj)	72.02 %	65.93 %	56.94 %
Cooling rate	Slower	Ref.	Faster
Sulf.	65.67 %	63 %	59.18 %
Sulf. (inj)	71.96 %	65.93 %	58.90 %
Sulf.^{M}	37.04 %	34.08 %	32.34 %
Sulf. (inj)^{M}	63.92 %	60.09 %	56.67 %
SO_3	Ref.	10 %	20 %
Sulf. (inj)	65.93 %	76.22 %	85.18 %
Sulf. (inj)^{M}	60.09 %	60.11 %	60.13 %

5
Conclusion

From the results presented in the previous Chapter it can be argued that the sulfation of alkali chlorides in Waste-to-Energy boilers can be predicted fairly well with one-dimensional simulations in CHEMKIN. However, more can be investigated and implemented to achieve a prediction model with more realistic assumptions. One such addition for the optimization would be to account for the impact from mixing and decomposition of SO_3 at the injection.

There are some main reasons for why it should not be possible to achieve an exact prediction with the method used in this thesis work. Firstly; the model does not account for variations in the temperature profile between the cases. However, it remains unknown how much the temperature profiles vary with time. Secondly; improper consideration of the mixing. The non-ideal mixing was attempted to be taken into account with the parameters X_S, X_{Cl}, $O_{2,inj}$ and CO_{inj}. There are better ways to take the mixing into account, for example by injecting sulfur and chlorine over time similarly to what was done with oxygen. To do this accurately however, more information would be needed about the mixing rate. The method with X_S and X_{Cl} was much easier to implement and served more as a crude way of realizing whether mixing was an important feature or not. Thirdly; averaged data. Mainly the data for the MEC boiler but also some data for the Renova boiler was to a certain extent averaged. This means that some variations between the cases cannot be predicted. One such averaged property that is believed to be the reason behind some of the variations between the cases is the hydrochloric acid content. Municipal solid waste (MSW) includes a large variety of different types of fuels such as plastic and wood. It is therefore very likely that the chlorine content in the fuel varies quite a lot with time and location in the fuel bed, leading to large variations in sulfation.

The model is, despite its' flaws, sufficiently accurately predicted the effects of variations in the process conditions. Some conclusions can be drawn with certainty from the model, such as the influence of temperature, chloride, sulfur and radicals. Other phenomena are less certain but the model still provides indications. For example, what causes variation in the experiments, how sulfuric acid decomposition and SO_3 impacts the sulfation, and how the flame actually progresses in the Renova boiler.

A suggestion for future studies is to investigate the distribution of elements in MSW. By knowing how alkali, chlorine and sulfur are released from the fuel bed the predictability of the model could be drastically improved. A statistical investigation of how the elements coexist in the flame could potentially be used to describe the

mixing. Additionally, it would be of interest to investigate how the sulfuric acid decomposes and is mixed with the flue gas when injected.

Bibliography

[1] T. Allgurén. *Chemical Interactions between Potassium, Nitrogen, Sulfur, and Carbon Monoxide in Suspension-Fired Systems*. PhD thesis, Department of Space, Earth and Environment, Chalmers University of Technology, Sweden, 2017.

[2] L. Hindiyarti, F. Frandsen, H. Livbjerg, P. Glarborg, and P. Marshall. An exploratory study of alkali sulfate aerosol formation during biomass combustion. *Fuel*, 87:1591–1600, 2008.

[3] S. Andersson, E. Blomqvist, L. Bäfver, F. Jones, K. Davidsson, J. Froitzheim, M. Karlsson, M. Larsson, and J. Liske. Sulfur recirculation for increased electricity production in Waste-to-Energy plants. *Waste Management*, 34(1):67–78, 2014.

[4] S. Andersson, E. Blomqvist, L. Bäfver, F. Claesson, K. Davidsson, J. Froitzheim, M. Karlsson, J. Pettersson, and B. Steenari. Sulphur recirculation for reduced boiler corrosion. Technical report, Waste Refinery, 2010.

[5] B. Sander. Properties of Danish biofuels and the requirements for power production. *Biomass and Bioenergy*, 12:177–183, 1997.

[6] A. Nordin. Chemical elemental characteristics of biomass fuels. *Biomass and Bioenergy*, 6:339–347, 1994.

[7] S. Karlsson, J. Pettersson, L.G. Johansson, and J.E. Svensson. Alkali Induced High Temperature Corrosion of Stainless Steel: The Influence of NaCl, KCl and CaCl2. *Oxidation of Metals*, 78:83–102, 2012.

[8] R. Gopalakrishnan and Mohindar S. Seehra. Kinetics of the high-temperature reaction of sulfur dioxide with calcium oxide particles using gas-phase Fourier transform infrared spectroscopy. *Energy Fuels*, 4:226–230, 1990.

[9] M. Steinberg and K. Schofield. The controlling chemistry of surface deposition from sodium and potassium seeded flames free of sulfur or chlorine impurities. *Combustion and Flame*, 129:453–470, 2002.

[10] K. Iisa, Y. Lu, and K. Salmenoja. Sulfation of Potassium Chloride at Combustion Conditions. *Energy Fuels*, 13:1184–1190, 1999.

[11] T. Taufiq. Characteristics of Fresh Municipal Solid Waste. Master's thesis, University of Texas at Arlington, 2010.

[12] C.P. Randolph and M.J. Overholster. The Emissivity of Oxidized Metallic Surfaces. *Phys. Rev.*, 2:144–152, 1913.

[13] S.E. Mörstedt and G. Hellsten. *Data och Diagram*. Liber AB, 7th edition, 2012.

[14] R. Johansson, B. Leckner, K. Andersson, and F. Johnsson. Account for variations in the H2O to CO2 molar ratio when modelling gaseous radiative heat

transfer with the weighted-sum-of-grey-gases model. *Combustion and Flame*, 158:893–901, 2011.

[15] S. Gharehkhani, A. Nouri-Borujerdi, S.N. Kazi, and H. Yarmand. Extension of Weighted Sum of Gray Gas Data to Mathematical Simulation of Radiative Heat Transfer in a Boiler with Gas-Soot Media. *The Scientific World Journal*, 2014:504601, 2014. doi: 10.1155/2014/504601.

[16] R.J. French, D.C. Dayton, and T.A. Milne. The direct observation of alkali vapor species in biomass combustion and gasification. Technical report, U.S. Department of Energy Office of Scientific and Technical Information, 1993.

[17] O. Dahl, H. Nurmesniemi, R. Pöykiö, and G. Watkins. Comparison of the characteristics of bottom ash and fly ash from a medium-size (32 MW) municipal district heating plant incinerating forest residues and peat in a fluidized-bed boiler. *Fuel Processing Technology*, 90:871–878, 2009.

[18] M. Li, C. Sun, S. Gau, and C. Chuang. Effects of wet ball milling on lead stabilization and particle size variation in municipal solid waste incinerator fly ash. *Journal of Hazardous Materials*, 174:586–591, 2010.

[19] Dominique Schwartz, Roger Gadiou, Jean-François Brilhac, Gilles Prado, and Ginès Martinez. A Kinetic Study of the Decomposition of Spent Sulfuric Acids at High Temperature. *Industrial & Engineering Chemistry Research*, 39(7):2183–2189, 2000.

[20] B. Andersson, R. Andersson, L. Håkansson, M. Mortensen, R. Sudiyo, and B. van Wachem. *Computational Fluid Dynamics for Engineers*. Cambridge University Press, 13th edition, 2017. Internal Chalmers version.

[21] Fluent Inc. 13.3.9 Choosing a Radiation Model, September 2006.

[22] W. Yan, H. Zhou, Z. Jiang, C. Lou, X. Zhang, and D. Chen. Experiments on Measurement of Temperature and Emissivity of Municipal Solid Waste (MSW) Combustion by Spectral Analysis and Image Processing in Visible Spectrum. *Energy Fuels*, 27:6754–6762, 2013.

[23] National Center for Biotechnology Information. PubChem Compound Database. Calcium Oxide, accessed Apr. 10, 2018.

A

Renova data

In Table A.1 below, the information gathered during the visit to Renova is presented. The information from the visit was used as a setup for the CFD-model, separate data for different cases were later used for in CHEMKIN. Note that the indices refer to Figure 3.2. Other data related to the process at Renova, such as heat capacities, enthalpies, mollier diagrams, could be obtained from the compilation by Mörstedt [13].

Table A.1: Monitored data gathered from the Renova boiler. * Corresponds to 20 °C and 1 bar. ** Corresponds to 0 °C and 1 bar. ^{D} implies on dry basis. ^{W} implies on wet basis.

Waste consumption	22 tonnes/h	
Steam production	68 tonnes/h	
Steam pressure	40.6 bar	
Superheated steam temperature	411 °C	
Turbine effect	24 MW	
Feedwater temperature	141 °C	
Steam drum pressure	50 bar	
Steam drum temperature	264 °C	
Primary air flow	78,000 m^3/h* ^{D}	
Primary air temperature	132 °C	
Secondary air flow	25,000 m^3/h* ^{D}	
Secondary air temperature	29 °C	
Recirculation air flow	21,000 m^3/h* ^{D}	
Recirculation air temperature	220 °C	
Total stack volume flow	106,000 Nm^3/h** ^{D}	
Volume fraction of O_2 in stack	0.095 ^{D}	
Volume fraction of CO_2 in stack	0.095 ^{D}	
Volume fraction of H_2O in stack	0.067 ^{W}	
Volume fraction of O_2 after combustion	0.063 ^{D}	
Volume fraction of H_2O after combustion	0.23 ^{W}	
Volume fraction of O_2 after ESP	0.085 ^{D}	
Top temperature	1093 K	Probe located at the top of the first channel
Final temperature	813 K	Probe located before the superheaters

B
Calculations

In this Appendix, the calculations for the Renova boiler as well as input data for the CFD-analysis is shown.

B.1 Calculations of Renova boiler flows

This section covers the equations necessary to calculate the flow properties for the Renova boiler using the gathered data. Since the data gathered from the Renova boiler was not generally inlet data, it needs to be refined before it can be used for the simulations in CHEMKIN and Fluent. Assuming ideal gas enables the use Equations B.1 and B.2 below.

$$PV = nR_gT \tag{B.1}$$

$$\text{mole fraction} = \text{volume fraction (wet basis)} \tag{B.2}$$

Where P is gas pressure, V is gas volume, n is moles of the gas, R_g is the ideal gas constant and T is gas temperature.

B.1.1 Treatment of data

Volume fractions based on dry gas can be converted to humid gas using Equation B.3 below.

$$X_k = X_{k,dry}(1 - X_{H_2O}) \tag{B.3}$$

In Equation B.3, X_k denotes the mole fraction of an arbitrary gas component. The molar flows can be calculated from the normalized volume flows using Equation B.4 below.

$$F_i = \frac{\dot{V}_i}{3600}\frac{P^{ref}}{T^{ref}R_g}\left(\frac{\sum_k^{N_k} X_k}{\sum_{k,k\neq H_2O}^{N_k} X_k}\right)^* \quad [kmol/s] \tag{B.4}$$

* The last term is only used if the volume flowrate are specified as dry

The equation to calculate the mole fraction of water in the flue gas is shown in Equation B.5 below.

$$X_{H_2O} = Y_{humid} \frac{\rho_{air}}{M_{H_2O}} \frac{T^{air} R_g}{P^{air}} * 1000 \tag{B.5}$$

B.1.2 Mass balances

This section includes the equations necessary to calculate the compositions and flow rates of the inlet flows and the flue gas. The total mass balance is shown in Equation B.7 below.

$$\sum_{i}^{N_{in}} F_i + R^* = \sum_{j}^{N_{out}} F_j \quad [mole/s] \tag{B.6}$$

Where R is the net production rate of number of moles. The component balance for species k is shown in Equation B.7 below.

$$\sum_{i}^{N_{in}} F_i X_{i,k} + R_k = \sum_{j}^{N_{out}} F_j X_{j,k} \quad [mole/s] \tag{B.7}$$

Where R_k is the production rate of species k in the unit. The sum of all mole fractions are by definition equal to unity according to Equation B.8 below.

$$\sum_{k}^{N_k} X_k = 1 \tag{B.8}$$

B.1.3 Energy balance

This section covers the equations needed to calculate the total heat duty achieved by the boiler. All temperatures were obtainable from the monitors and they are defined in Kelvin in the equations below. The heat output from the boiler before the superheaters is calculated with Equation B.9 below.

$$Q_{steam} = \frac{\dot{m}_{steam}}{3.6} (\Delta H_{vap} + C_{p,H_2O}(T_{sat} - T_{in})) \quad [kW] \tag{B.9}$$

To account for the losses to the ambiance an efficiency factor had to be estimated. The losses were assumed to occur due to heat conduction in the insulation material Mineral wool according to Data & Diagram [13] with a thickness (d) of 30 cm and assuming the outside surface temperature (T_{walls}) was 50 °C. The efficiency (η) was calculated according to Equation B.10 below.

$$\eta = \frac{A_{walls} * \lambda_{wool} * (T^{sat}_{steam} - T_{walls})}{d * Q_{steam}} \tag{B.10}$$

The estimated temperature in the incinerator assuming heat capacity at 1000 °C and that all reactions occur instantly, no heating of non-burnables, steady state and energy conservation was calculated with Equation B.11 below. Note that this was only used as a preliminary inlet temperature for the CFD model, after which the method described in Section B.2.3 was used.

$$T_{incineration} = \frac{Q_{steam}}{\sum_k^{N_k} X_{RG,k} C_{p,k,1000°C}} + T_{superheaters} \quad [K] \tag{B.11}$$

B.1.4 Waste

The water in the flue gas stream can be assumed to originate from 4 different sources; humidity in the air from the inlets, humidity in the recirculation stream, production due to the combustion and moisture in the waste. The first two were solved by using mass balances while the last could be assumed to make up the excess water. The production due to the combustion process must however be calculated assuming conservation of elements, namely oxygen. This contribution was calculated according to Equation B.12 below.

In order to calculate the amount of water produced from the combustion, a material balance was done over the oxygen in and out of the system. Two moles of water is formed for every mole of oxygen that has not either turned into carbon dioxide or remained unreacted. Since there is carbon dioxide in the recirculation stream, it must be taken into account. The resulting balance can be seen in Equation B.12 below where F_i is the molar flow of stream i in Figure 3.2.

$$F_{3,H_2O,Comb} = 2 * \left((F_1 + F_2) * X_{air,O_2} + F_6 * X_{6,O_2} + F_6 * X_{6,CO_2} - F_3 (X_{3,O_2} - X_{3,CO_2}) \right) \tag{B.12}$$

The equation for the calculation of the moisture content in the waste can be seen in Equation B.13 below where $\dot{m}_{waste}$ for the boiler at Renova was approximately 22 tonnes per hour.

$$Y_{moisture} = \frac{F_{3,H_2O,moist} * M_{H_2O}}{\dot{m}_{waste}} \tag{B.13}$$

B.2 Input data for CFD

Before the CFD-analysis was initiated, data was needed regarding inlets and fluid properties. This section will briefly cover the calculations made to achieve these data.

B.2.1 Flue gas composition

Through the processes described earlier in this section along with the data presented in Section A, the composition of the flue gas, when the combustion has occurred, could be calculated. The composition of the flue gas was used to define the properties for the fluid in the CFD-model and can be seen in Table B.1 below.

Table B.1: Composition of flue gas in mole-basis.

Specie	Concentration
O_2	4.85 %
H_2O	23.00 %
CO_2	9.37 %
N_2	62.78 %

B.2.2 Heat conduction

For a wall made up of more than one material, the effective heat conductivity can be calculated according to Equation B.14 [13]. This was done for the boiler walls since the impact of the deposits should be taken into account.

$$\lambda_{wall} = \frac{L_{wall}}{\sum_i \frac{L_i}{\lambda_i}} \tag{B.14}$$

B.2.3 Inlet temperature correction

The preliminary inlet temperatures were calculated with the total heat duty of the boiler and the outlet temperature according to Equation B.11 in Section B.1.3. This inlet temperature needs to be corrected to account for the contribution from the radiation. This was done after all other simulation parameters had been investigated and verified and several preliminary simulations had been run. Using what is known from preliminary simulations, i.e. heat into the walls, radiation and simulated inlet temperature, it was possible to estimate the representative inlet temperature with radiation included using Equation B.15 to solve for T_{in}.

$$\frac{Q_{steam}}{\eta_{steam}} - Q_{walls,s} = \dot{m}C_p(1750K)(T_{in} - T_{in,s}) + C * T_{in}^4 - C * T_{in,s}^4 \tag{B.15}$$

where index s implies the previous simulation results, η is efficiency calculated in Section B.1.3 and C is defined in Equation B.2.3 below.

$$C = \frac{Q_{walls,s} - \dot{m}(H_{in,s} - H_{out,s})}{T_{in,s}^4}$$

Using previous simulation results along with Equation B.15 the temperature was predicted to be 1484K, which was then used as the inlet temperature in the CFD-model.

C

CFD analysis

In this Appendix the methodology that was used for the CFD analysis will be presented more thoroughly. The objectives were to find a realistic temperature profile as well as residence time for the flow to use in CHEMKIN. A fair amount of models and assumptions are discussed and implemented.

C.1 Geometry

A CAD geometry of the Renova boiler was created in the DesignModeler program in Ansys workbench. In order to create the geometry; three drawings with the needed dimensions and angles were provided by Renova and measured on site. The finished geometry can be seen in Figure C.1 below.

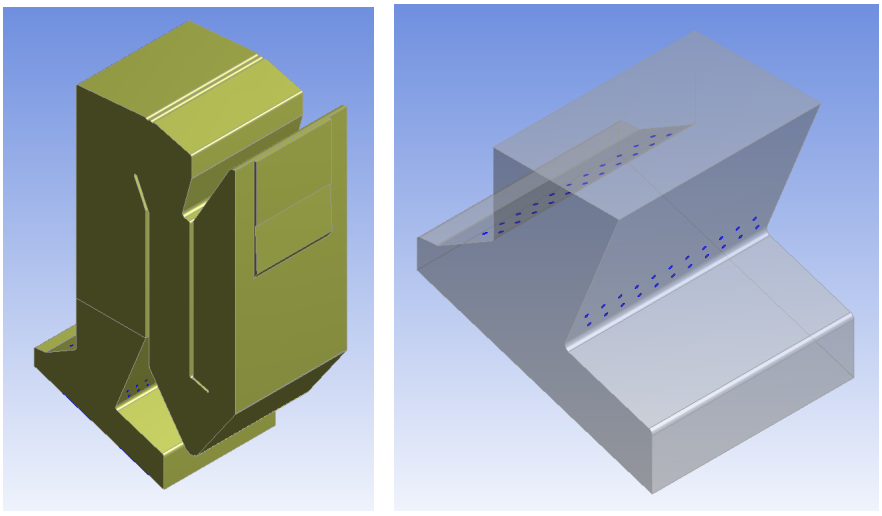

(a) The whole boiler. **(b)** The inlets of the boiler.

Figure C.1: 3D Geometry of the boiler which was used in the CFD-model.

C.2 Meshing

The mesh for the geometry was conducted in the Fluent meshing program. At first; a course mesh was created so that a finer mesh could be created gradually. The

first mesh contained about three hundred thousand tetrahedral cells. It was discovered that it was much easier to achieve an even mesh when using tetrahedral cells instead of hexahedral cells. After all refinements had been done, the mesh had approximately 1.6 million cells.

When using wall functions, it is assumed that the flow is in local equilibrium, i.e. production equals dissipation. This assumption is valid in the fully turbulent sublayer which corresponds to y^+ values above 30. However, the y^+ values must not be too high either since the error of the wall functions then will increase [20]. By starting off with a very coarse mesh and then refine it successively where the y^+ values are extremely high, an acceptable wall mesh was achieved. Figure C.2 below shows the y^+ values at the walls for the refined mesh. It can be seen that most of the y^+ values are in an acceptable range. Furthermore, those that are not was considered not to have a significant impact on the simulations due to their positions. This is because most locations that have a y^+ value below 30 is corners in the lower region of the boiler where the flow rate is very low and where flow patterns and/or temperatures are not important for the outcome of the model.

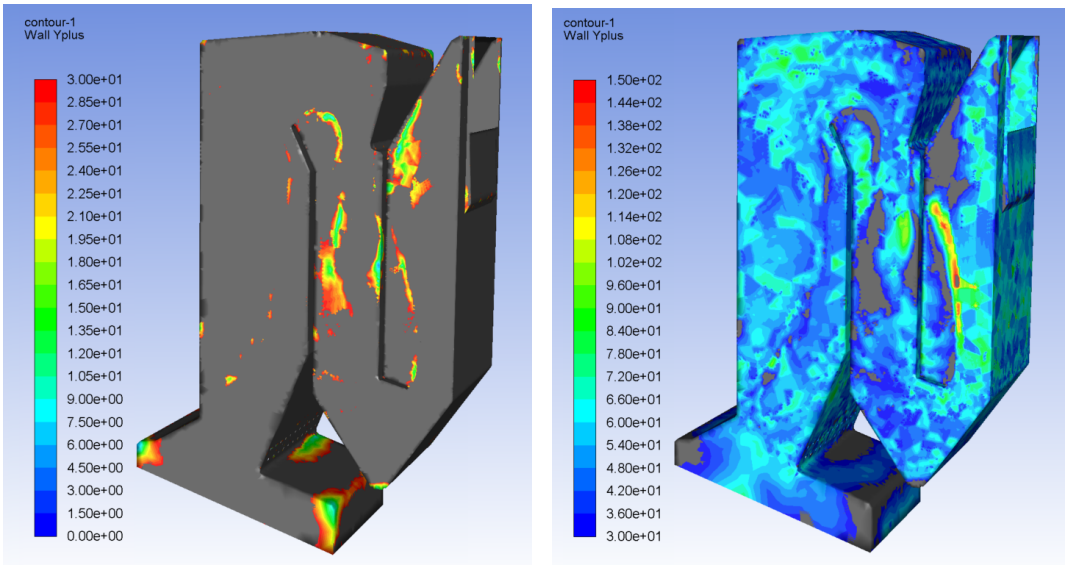

(a) y^+ values between 0 and 30. **(b)** y^+ values above 30.

Figure C.2: y^+ values.

To make sure that the solution does not depend on the size of the mesh, a mesh independence analysis was performed. This was done in Fluent by refining the mesh where the curvatures of velocity and temperature were large. By doing this until the solution no longer changed, mesh independence could be proven. Important to note is that the variations in the checked parameters decreased with each refinement which means that the absolute values from the first iterations are not as credible as from the latter.

C.3 Inlet- and boundary conditions

The walls of the boiler are made of a 5 mm thick steel wall with boiling water on the outside with a temperature of 263.9 °C. The walls in the combustion area are also covered with a 5 cm thick concrete wall. All walls inside the boiler are assumed to be covered by an evenly distributed layer of deposits created due to the salts in the fuel. The thickness of the deposits is used as a design variable to reach the correct temperature in the outlet of the boiler.

For steel, concrete and deposits the only properties of interest are heat conductivity and emissivity since they are the only relevant properties to transport heat out of the system for a steady solution. All other material properties are set according to the standard values present in Fluent except for the emissivity which will be discussed in the next section. The heat conductivity for steel was set according data for steel within the software, a value which was compared to literature data [13]. For the concrete wall the heat conductivity was found to be 9 $Wm^{-1}K^{-1}$. The heat conductivity for the deposits was set to 1 $Wm^{-1}K^{-1}$ according to similar materials found in literature [13]. Since the materials are layered, the thicknesses are summed according to Equation B.14.

The volume flows are defined in Table A.1 for all the inlets along with their actual inlet temperatures. All of the secondary and recirculation inlets were angled differently and this was implemented in the model. The flow of the primary inlets was assumed to be directed upwards. The temperatures had to be modified to include the heat of the reaction in the CFD model which was described in Appendix B.2.3.

All inlets were assumed to inject air with modified properties. The simulation did not account for species transport in any way. The kinetic theory of gases was used to model the viscosity and thermal conductivity of the flow.

C.4 Radiation

Radiation is the dominant heat transfer phenomenon in the boiler up until the superheaters where convection becomes dominant. It was modeled with the discrete ordinates (DO) model. The reason why this was chosen is because it should work well for problems with localized heat sources such as the burning waste in this case. The boiler is also rather large which suggests that the optical thickness is much bigger than unity, this is another indicator that the DO-model should be used for this case [21].

The emissivity of the burning solid waste was initially set to 0.95 which corresponds to the measurements made by Yan et. al [22]. These data were measured on a similar waste incinerator as the one simulated in this project. However after realizing that the peak temperature should not be at the inlet, this was set to zero

to counter the effect. The emissivity of the steel walls was set to 0.79 which is based on measurements made on oxidized steel at 600 ^{o}C [12]. This is close to the temperature of the steel walls inside the boiler.

The radiative properties of the gas almost exclusively comes from the contribution of the CO_2 and water vapour and was implemented into the CFD-model as an absorption coefficient. This coefficient was modelled using a WSGG model (Weighted Sum of Grey Gases) which should be applicable for the H_2O/CO_2 fraction and temperature range of the Renova boiler [14].

The radiative properties of the soot particles in the boiler at Renova have been found to depend on temperature and concentration. A simple term was calculated and included in the WSGG model mentioned above from the work by Gharehkhani et al. [15]. The term was then implemented into the CFD-model as a function of temperature.

C.5 Results

The resulting temperature contour and the pathlines for the fluid can be found in Figure C.3 below. For information of what these results were used for, see Appendix D

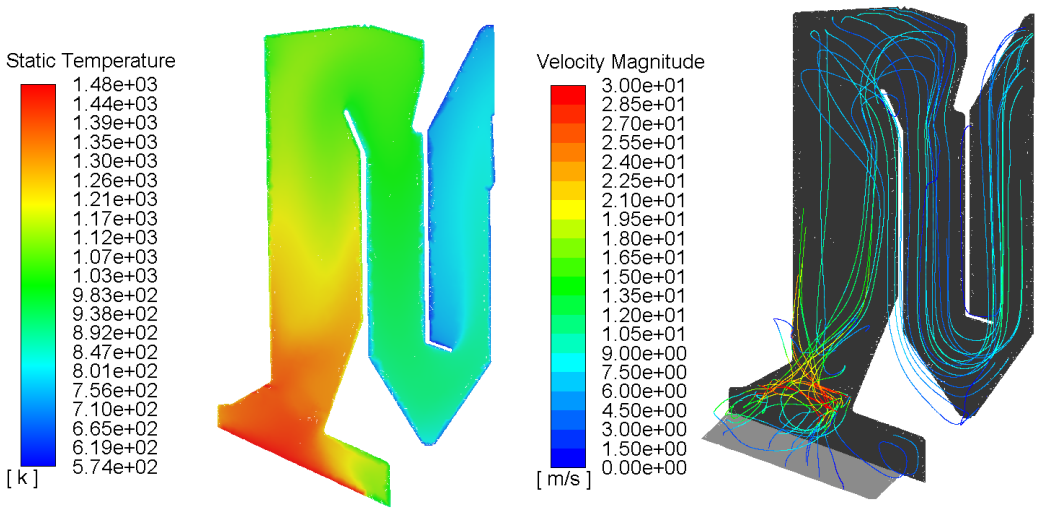

(a) Temperature in the Renova boiler. **(b)** Pathlines with the velocity magnitude for the Renova boiler.

Figure C.3: CFD results.

D

Data Processing

The objective of this chapter is to describe the methodology that was used to average the temperature curves from CFD using MATLAB.

D.1 Temperature profiles

The pathlines for temperature versus time was retrieved from the CFD-simulation and the temperatures could be plotted against time to give an indication of the cooling progression of the flue gas through the boiler. Figure D.1 below shows 15 temperature profiles out of the total 1131 retrieved pathlines.

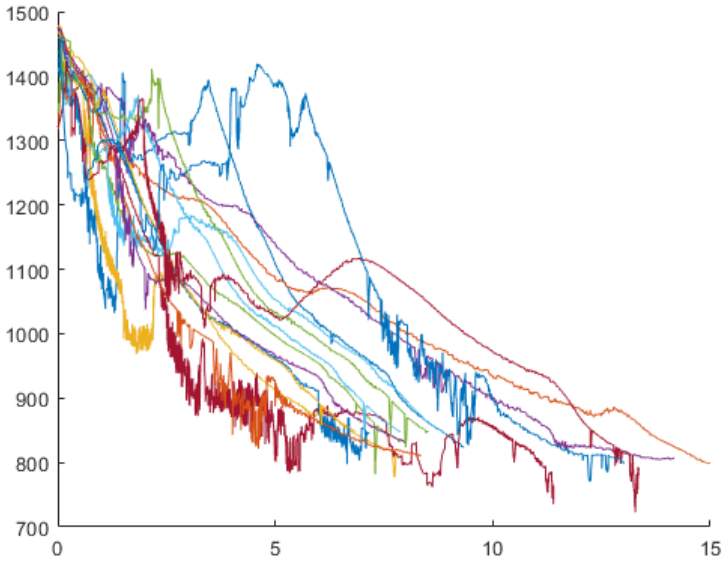

Figure D.1: Temperature of 15 pathlines against time.

Before anything was further done, the few pathlines that got stuck in loops and never left the system were removed to avoid nonphysical influence of statistics. 21 outliers were removed out of the total 1131 pathlines, which corresponds to 1.8568 %.

In addition to the temperature profiles, a pathline file was extracted from the CFD-results. The time and vertical coordinate of these pathlines could then be analyzed which made it possible to know which pathlines originates from which primary inlet

so that they could be scaled depending on the flow rate of their respective inlet as well as the amount of pathlines that have the same inlet origin. The vertical coordinate of the pathlines could also be used to define the time of the SO_2-injection assuming SO_2 was injected at a plane, 11 meters above the boiler inlet. The general injection- and the residence times of the pathlines can be seen in Figure D.2 below.

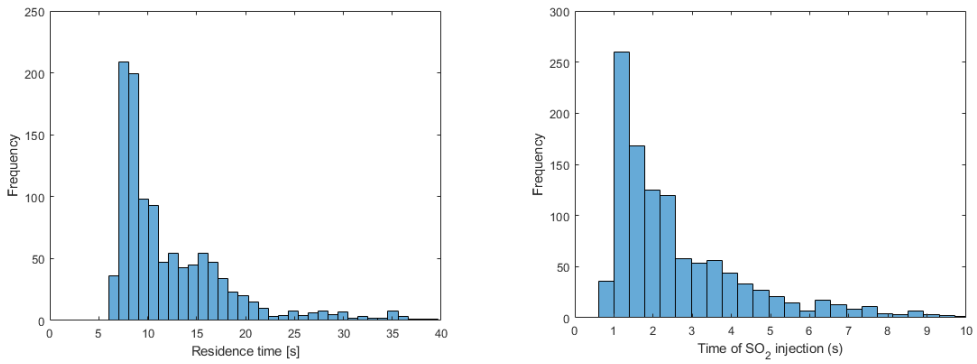

(a) Histogram of residence time.

(b) Histogram of time of SO_2-injection.

Figure D.2: Histograms of the pathlines revolving time.

D.2 Temperature profile averaging

The temperature profiles that were obtained in the CFD-model needed to be represented so that the number of simulations in CHEMKIN could be reduced. The following methods were tried and tested:

- Averaging temperature based on time.
- Averaging time based on temperature.
- Averaging derivative based on temperature or time.
- Averaging angle of change based on temperature or time (from -90°to +90°)
- Averaging polynomials fit to each temperature curve.
- Averaging residence time within temperature intervals.

Some attempts included more than one curve, in which case the different curves were usually separated based on residence time or average cooling rate. A problem that often presented itself was to get the data to the same point, i.e. creating intervals and defining data within these intervals together. When averaging based on time it proved necessary to include all temperature curves even after they have exited the boiler as their exit temperature. If this was not done then the temperature took a small leap up when the curves exited the system which lead to the average not going below 1000 K which is not realistic.

The most realistic method turned out to be averaging temperature based on time where the curve ends at the median residence time, 10.18 seconds. The resulting

curve was used and can be seen in Figure 3.6a. Another method was to average the residence time within temperature intervals which gave a more linear looking curve. This resulted in higher rates of sulfation when directly implemented in CHEMKIN but an unnatural cooling rate.

E

CHEMKIN clarification

The purpose of this chapter is to provide some background knowledge and clarification regarding the assumptions for the CHEMKIN simulations.

E.1 Source terms

The figures in this section display simplified depictions of where the source terms were active and to what extent. Figure E.1 below shows the source term for carbon monoxide used in the 1D CHEMKIN simulations. The rest of the carbon monoxide enters at the inlet and in total this results in the total expected carbon dioxide at the outlet. The background for this assumption is that there is no complete combustion of carbon monoxide in the flame. Carbon monoxide is therefore injected after the flame and oxidized instantly when it enters the reactor. This method allows the carbon monoxide to oxidize at a small rate throughout the whole boiler which is necessary due to non ideal mixing.

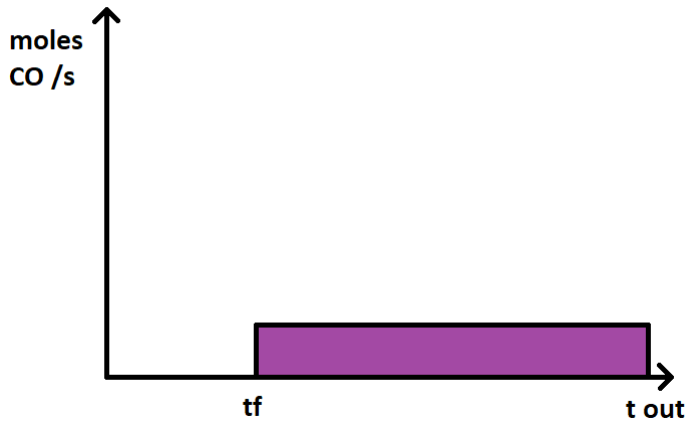

Figure E.1: Simplified source term graph for carbon monoxide. In the reference setup it is 1 % of the total carbon monoxide at the outlet that originates from this source term, i.e. $CO_{inj} = 1\%$.

Figure E.2 below shows the injection for the oxygen used in the 1D CHEMKIN simulation. The amount of added oxygen can be seen in Table 3.1 and the sum of the added oxygen is supposed to cover the oxidation of hydrogen into water as well as carbon monoxide into carbon dioxide. Additionally, there should be approximately 5 % oxygen remaining after boiler.

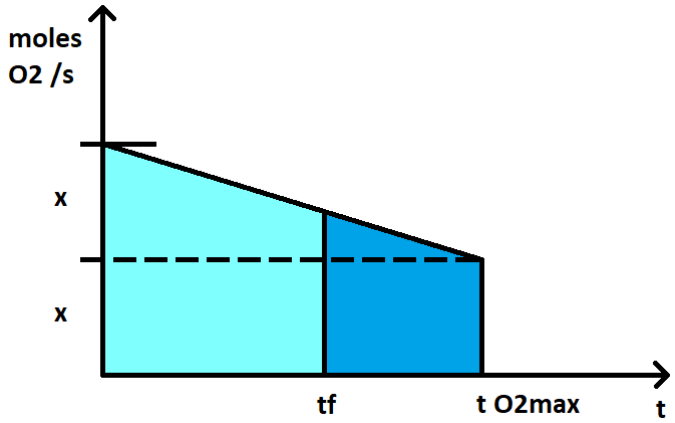

Figure E.2: Simplified source term graph for oxygen. The shape is defined as a triangle on top of a rectangle which both have the same side x. The area to the right of t_f is the proportion of the oxygen that remains unreacted after entering the PFR. This propotion together with the t_f defines the $t_{O2,max}$

Figure E.3 below shows the source term that is used to produce the temperature profile for Renovas boiler which can be seen in Figure 3.7a. Ts in this figure is varied together with a factor for the cooling rate to fit the outlet temperature and energy balance. For more information, see Section 3.3.

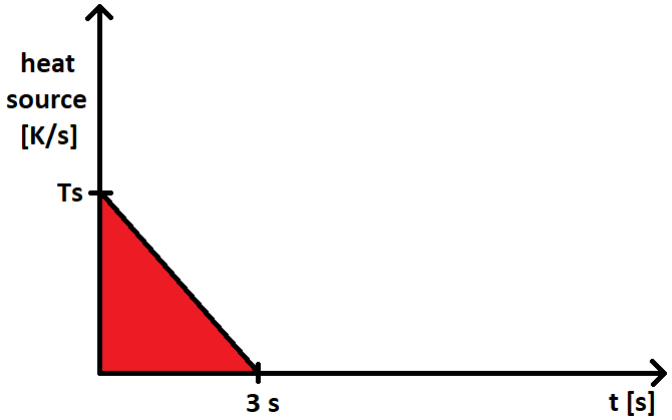

Figure E.3: Heat source for Renovas boiler in units Kelvin per seconds.

E.2 Calcium oxide reaction with sulfur

All calcium apart from the calcium sulfate originating from fuel can be assumed to be calcium oxide. Other compounds such as calcium carbonate quickly reduces to calcium oxide while combustion occurs, according to Seehra and Gopalakrishnan [8]. In the same paper, some kinetic terms regarding the sulfation process of porous particles of calcium oxide are proposed, such as the ones that can be found in waste incineration. Equations E.1, E.2 and E.3 can be used to describe the kinetics with the parameters defined by Seehra and Gopalakrishnan [8] in Table E.1 below.

Table E.1: Parameters for Equation E.1 within the temperature range 700°C to 1000 °C.

	Without oxygen	With oxygen
$A,\ g^2/(m^4\ Torr\ s)$	243.0	3571.7
m	0.6	0.6
$E,\ kcal/mol$	26.2	34.7

$$k_d = AS^2 p^m e^{\frac{-E}{RT}} \tag{E.1}$$

where p is partial pressure of SO2 in the system and

$$S = \frac{3}{\rho r} \tag{E.2}$$

where ρ is the density of calcium oxide, which according to Pubchem [23] is 3340 kg/m^3 and r is the radius of the particle which is found by Sun et al. [18] to be approximately 50 µm. The rate constant in Equation E.1 can at any given temperature then be translated into conversion of CaO through Equation E.3 along with duration, t [s]. Note that the term $k_d t$ is assumed to be additive meaning it is possible to add together different temperatures with duration.

$$k_d t = 1 - 3(1 - X_{CaO})^{2/3} + 2(1 - X_{CaO}) \tag{E.3}$$

By combining the temperature profile in Figure 3.5a with the Equations E.1, E.2 and E.3 it is possible to retrieve the resulting conversion of calcium oxide in the boiler. The parameters for the scenario without oxygen in Table E.1 was used up until the peak temperatures in the temperature profile, after which the parameters for abundant oxygen were used. However, using the radius mentioned by Sun et al. [18], none of the 9 Renova cases yielded a conversion above 1%. Despite lowering the radius to as low as 10 µm, the conversion still never reached 2%. If not even this drastic change in radius would improve the slow reaction rate then it is highly probable that this reaction is too slow to consider in the simulated boilers.